Universidade de Aveiro
2022

Gonçalo Pratas Lima Da Costa

Análise Biomecânica Comparativa do Disco Cervical Intervertebral Nativo e Prostético

Biomechanical Analysis and Comparison of the Native and Prosthetic Cervical Intervertebral Disc

Universidade de Aveiro
2022

Gonçalo Pratas Lima Da Costa

Biomechanical Analysis and Comparison of the Native and Prosthetic Cervical Intervertebral Disc

Análise Biomecânica Comparativa do Disco Cervical Intervertebral Nativo e Prostético

Thesis submitted to Universidade de Aveiro (University of Aveiro) in order to satisfy the necessary requirements for the Master's Degree in Biomedical Engineering, performed under the scientific orientation of Professor António Manuel de Amaral Monteiro Ramos of the Mechanical Engineering Department of the University of Aveiro and co-oriented by Professor Michel Mesnard of Institut de Mécanique et d'Ingénierie of the Université of Bordeaux.

Dissertação apresentada à Universidade de Aveiro para cumprimento dos requisitos necessários à obtenção do grau de Mestre em Mestrado Integrado em Engenharia Biomédica, realizada sob a orientação científica do Professor Doutor António Manuel de Amaral Monteiro Ramos do Departamento de Engenharia Mecânica da Universidade de Aveiro e co-orientada pelo Professor Doutor Michel Mesnard do Institut de Mécanique et d'Ingénierie da Université de Bordeaux.

Esta dissertação teve o apoio dos projetos PTDC/EME-EME/32486/2017, UIDB/00481/2020, UIDP/00481/2020 - Fundação para a Ciência e a Tecnologia; e CENTRO-01-0145 FEDER-022083 - Programa Operacional Regional do Centro (Centro2020), através do Portugal 2020 e do Fundo Europeu de Desenvolvimento Regional.

To my family and friends

o júri/ the juri

President / president	Professora Doutora Ana Luísa Monteiro da Silva Professora Auxiliar em Regime Laboral, Universidade de Aveiro
vogal / examiner	Doutor José António de Oliveira Simões Equiparado a Professor Coordenador C/ Agregação, ESAD - Escola Superior de Artes e Design de Matosinhos
orientador / supervisor	Professor Doutor António Manuel de Amaral Monteiro Ramos Professor Auxiliar, Universidade de Aveiro

agradecimentos/ acknowledgements

I would like to thank my teacher António Ramos for his dedication, patience, availability and helpfulness in doing this work which was only possible with his help.
I would also like to thank Professor Michel Mesnard for the advice and helpfulness in accomplishing the objectives of this study.
Thank you also to my friends and teachers for accompanying me in my university journey.

palavras-chave

Coluna Cervical, Biomecânica, Disco intervertebral, Artroplastia, Implantes Discais, Deformação.

resumo

O objetivo principal deste trabalho é realizar uma análise biomecânica comparativa entre o disco intervertebral natural (IVD) e o disco artificial prostético na coluna cervical.

A coluna cervical é uma estrutura complexa e essencial que fornece movimento e estabilidade para além de proteger a medula espinhal. A coluna vertebral inclui várias estruturas, incluindo as vértebras, os IVDs, tecidos nervosos e ligamentos. A coluna cervical pode realizar vários movimentos da cabeça que incluem a extensão, flexão, flexão lateral e rotação axial. Diferentes forças são aplicadas em diferentes direções devido aos músculos, ligamentos e peso de diferentes estruturas. Com uma lesão na coluna ou apenas com o envelhecimento, podem ocorrer patologias da coluna vertebral, como doença degenerativa do disco (DDD) e hérnia de disco traumática. Essas doenças fazem com que o IVD perca sua integridade causando dor e perda de flexibilidade. Existem vários tratamentos, incluindo a substituição total do disco por um disco prostético. Existem vários modelos destes dispositivos e cada um tem seus benefícios e desvantagens. Neste trabalho o disco Mobi-C foi utilizado para comparar suas propriedades biomecânicas com o disco natural. Há uma escassez de estudos que fazem essa comparação, mas existem vários estudos que mostram o comportamento compressivo do disco natural e protético separadamente.

Um modelo experimental foi criado para imitar a coluna cervical em uma máquina de tensão compressiva para testar o disco natural e prostético. As vértebras C5 e C6 foram escolhidas para este estudo por serem aproximadamente semelhantes em estrutura e por estarem localizadas na parte inferior da coluna cervical onde as cargas aplicadas são maiores. Diferentes materiais são usados neste sistema, incluindo as vértebras, peças de suporte, o disco Mobi-C, um modelo de disco natural, ligamentos e sensores strain gauges tri-axiais. O conjunto permite a posição neutro, flexão de 10 graus e extensão de 10 graus da coluna. Sensores strain gauge foram utilizados para avaliar strain nas facetas anterior e posterior do corpo vertebral de cada vértebra. Três discos naturais diferentes com três valores de dureza diferentes foram testados e comparados entre si. Um disco natural foi escolhido para comparar com o disco protético. Ambos os modelos foram avaliados para diferentes posições da coluna vertebral dando valores máximos e mínimos de deformação para cada sensor ($\boldsymbol{\varepsilon_{max}}$ e $\boldsymbol{\varepsilon_{min}}$).

Ao comparar os modelos natural e prostético, concluiu-se que a montagem com os discos naturais distribui a carga aplicada ao sistema de forma menos uniforme pelo corpo vertebral do que o disco prostético. A diferença entre o maior valor de strain e o menor é 520,76 µm/m e 0,59 µm/m para $\boldsymbol{\varepsilon_{max}}$ e $\boldsymbol{\varepsilon_{min}}$ no modelo de disco natural e 207,31 µm/m e 274,77 µm/m para $\boldsymbol{\varepsilon_{max}}$ e $\boldsymbol{\varepsilon_{min}}$ no modelo do disco prostético. A disparidade entre os valores nos diferentes sensores é visivelmente maior no disco natural do que no disco prostético. Isto deve-se principalmente à geometria, propriedades mecânicas e a posição do disco prostético neste sistema experimental o que pode indicar benefícios para o tratamento de patologias da coluna vertebral.

keywords

Cervical Spine, Biomechanics, Intervertebral Disc, Arthroplasty, Prosthetic Disc, Deformation

abstract

The main objective of this study is to build a biomechanical analysis and comparison between the natural intervertebral disc (IVD) and the artificial prosthetic disc on the cervical spine.

The cervical spine is a complex and essential structure that provides motion and stability while also protecting the spinal cord. The spine includes several structures including the vertebrae, the IVDs, nervous tissues, and ligaments. The cervical spine can perform several movements of the head which include extension, flexion, lateral bending and axial rotation. It has different forces applied in different directions due the muscles, ligaments and weight of different structures. With an injury in the spine or just with aging, spinal pathologies such as degenerative disc disease (DDD) and traumatic disc herniation can occur. These diseases cause the IVD to lose its integrity causing pain and loss of flexibility. Several treatments exist including total disc replacement with a prosthetic disc. There are several models of these devices and each one has its benefits. In this work the Mobi-C was used to compare its biomechanical properties to the natural disc. There is a scarcity of studies doing this comparison but there are several studies that show the compressive behaviour of the natural and prosthetic disc separately.

An experimental model was created to mimic the cervical spine in a tensile tester machine to test the natural and prosthetic disc. The C5 and C6 vertebrae were chosen for this study because they are similar in structure, and they are located in the lower part of the cervical spine where loads applied are higher. Different materials are used in this system including the vertebrae, support pieces, the Mobi-C disc, a natural disc model, ligaments and tri-axial strain gauges. The assembly can mimic the neutral, flexion of 10 degrees and extension of 10 degrees of the spine. Strain gauge sensors were used to evaluate the deformation in the anterior and posterior facets of the vertebral body of each vertebra. Three different natural discs with three different hardness values were tested and compared with each other. One natural disc was chosen to compare with the prosthetic disc. Both models were assessed for different positions of the spine giving maximum and minimum values of principal strain for each sensor ($\boldsymbol{\varepsilon_{max}}$ and $\boldsymbol{\varepsilon_{min}}$).

When comparing the natural and prosthetic models, it was concluded that the assembly with the natural discs distribute the load applied to the system less evenly across the vertebral body than the prosthetic disc. The difference between the highest strain value and the lowest is 520.76 µm/m and 0.59 µm/m for $\boldsymbol{\varepsilon_{max}}$ and $\boldsymbol{\varepsilon_{min}}$ in the natural disc model and 207.31 µm/m and 274.77 µm/m for $\boldsymbol{\varepsilon_{max}}$ and $\boldsymbol{\varepsilon_{min}}$ in the prosthetic disc model. The disparity between values in different sensors is noticeably higher in the natural disc than in the prosthetic disc. So, the main conclusion was that the prosthetic disc distributes the load of the cervical spine in a more uniform distribution on the vertebral body of the vertebrae than the natural disc model due mainly to its geometry, mechanical properties and position in this experimental assembly which suggests benefits for treating spinal pathologies.

Contents

List of Figures

Chapter 1. The Cervical Spine

In this chapter, the cervical spine is introduced including its anatomy and its biomechanics which will serve as a basis for this study. Pathologies of the cervical spine are also explored along with current treatment options.

1.1. Anatomy of the cervical spine

The human spine is the main support system of the human body. It is a complex and essential structure that provides motion and stability while also protecting the spinal cord. The whole structure can be divided into four main sections: the cervical spine, the thoracic spine, the lumbar spine, and the sacrum. The neck encompasses the region between the base of the head and the thoracic inlet [1]. This project will focus on this area of the cervical spine, providing insight into how the different components behave biomechanically.

Figure 1.1 Lateral view of the cervical spine [2]

The cervical spine involves several structures including the vertebrae, the intervertebral discs (IVDs), nervous tissues, and ligaments. Each structure is composed of a unique biomaterial with particular biomechanical qualities like hardness and deformation. For example, the vertebrae are made of hard bone material while the IVDs are made of elastic soft tissues [1].

The cervical spine is comprised of seven vertebrae named from C1 to C7 from top to bottom. C1 and C2 also called Atlas or Axis have specific geometries; they are responsible for most of the rotation and flexion of the head. The C3 to C6 vertebrae follow the same basic anatomical structure. As seen in figure 1.2A they have a body that occupies most of the anterior part of the structure, the lamina, the vertebral arch, and the posterior spinous process located at the posterior section. They are positioned in a way that allows the spinal cord to pass through the posterior part of the spine. The vertebral body supplies strength and support for two-thirds of the vertebral load. The endplates of the body are concave laterally and convex in an anterior-to-posterior direction. The depth of the inferior endplate of the vertebral body is larger than the depth of the superior endplate in the C3 to C6 segment. These endplates are where the disc is connected which permits articulation with the adjacent vertebra.

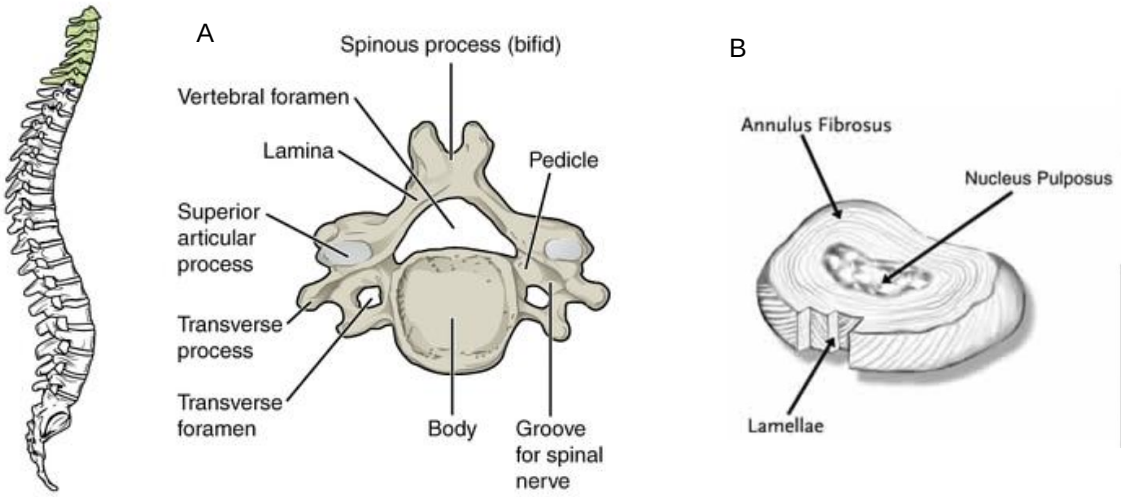

Figure 1.2 A-Anatomy of the typical cervical vertebra. B-Anatomy of the natural IVD [3], [4].

IVDs allow the movement of the cervical spine due to their mechanical properties. They have a two-part structure, the annulus fibrosus, and the nucleus pulposus. In figure 1.2B it is possible to see that the nucleus pulposus is the inner

part of the disc surrounded by the annulus fibrosus. The nucleus is formed of a gelatine-like substance composed of 88% water, collagen fibres, and chondrocyte-like cells. The annulus fibrosis are the outer shell of the disc and it is composed of concentric fibber layers of collagen and proteins (lamellae) [1], [5].

Spinal ligaments surround the cervical spine to stabilize, protect and control its movement. As illustrated in figure 1.3, the ligaments are divided into six groups according to their location:

- Anterior longitudinal ligaments - set on the anterior facet of the vertebral bodies
- Posterior longitudinal ligaments - set on the posterior facet of the vertebral bodies
- Ligamentum Flavum - join the lamina of one vertebra to the lamina of the adjoining vertebra
- Capsular ligaments - join the inferior articular surfaces of a vertebra with the superior articular surfaces of a vertebra directly below it to the side
- Interspinous ligaments - join the spinal process of one vertebra to another
- Supraspinal ligaments - are set on the posterior surfaces of the vertebra's spinal process [6].

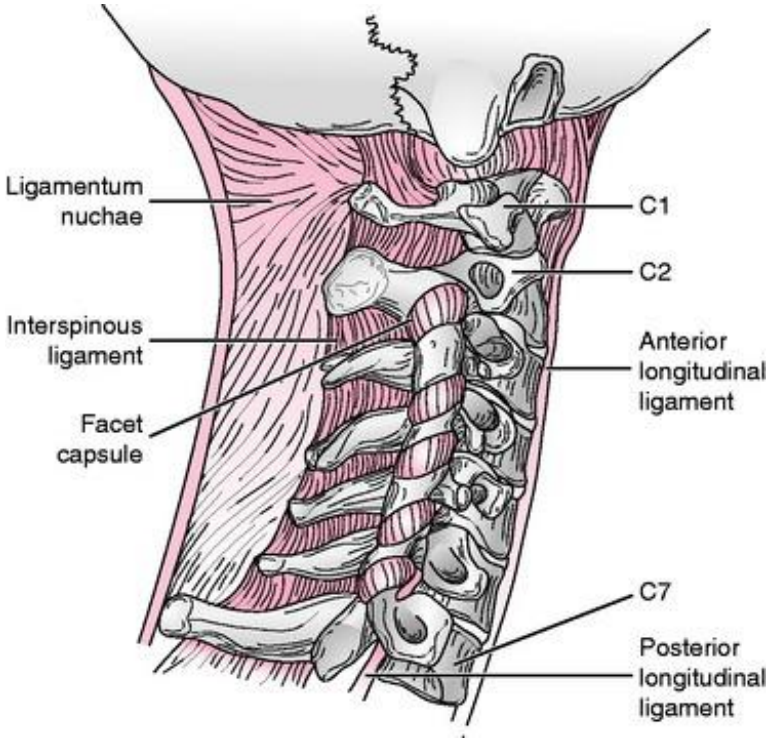

Figure 1.3 Supporting ligaments of the cervical spine [7].

1.2. Biomechanics of the cervical spine

It is important to understand the biomechanics of the cervical spine to study the forces and corresponding deformations that happen in the different components.

The movement of the neck and the head depends on the cervical spine and its articulations. To better understand movement and force directions three main plains are commonly used as reference points: the frontal or coronal plane, the sagittal or median plane and the horizontal or transverse plane. There are four principal movements of the neck as shown in figure 1.4:

- Flexion: moving the head to the anterior part of the body
- Extension: moving the head to the posterior part of the body
- Rotation: rotating the head left and right
- Lateral flexion: bending the head to the left and right

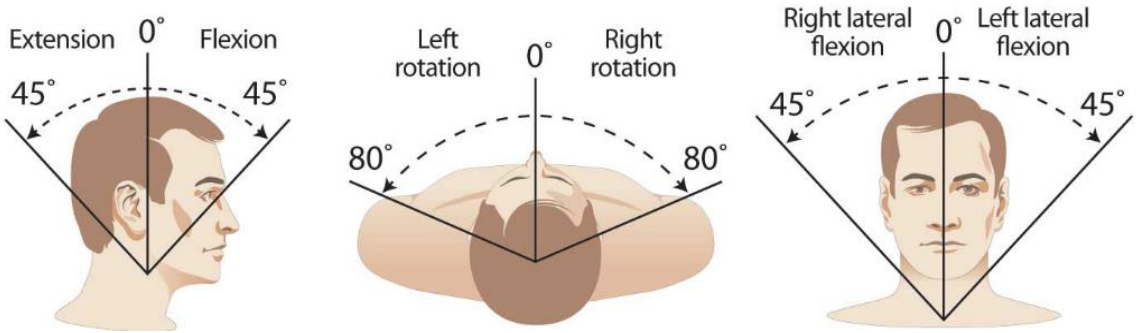

Figure 1.4 Approximate ranges of different neck movements [8].

The head of the patient is in equilibrium with the neck when the body is in the upright static position. The cervical spine is not vertical, it is curved. This natural curvature of the cervical spine is known as natural cervical lordosis. Usually, males have larger median cervical lordosis than females (20 and 14 degrees respectively). By comparing profile x-rays during maximum flexion-extension it's possible to deduce that the total range of flexion-extension of the inferior cervical spine is from 100-110 degrees and the total range of flexion-extension of the whole of the cervical spine is around 130-140 degrees. Each IVD is responsible for partial movement in the neck mobilization. In table 1, the average range of flexion and extension is shown [9]–[11].

The typical human head weighs an average of 4 to 5 kilograms which equals approximately 40 to 50 newtons of force on the spine. Along with the weight of the head, muscles and ligaments create two types of forces applied in the cervical spine: compressive and shear. In figure 1.5 compressive forces are shown for different movements of the neck. The lowest and highest biggest compressive loads are present in the C0/C1 articulation (14% body weight) and C7/T1 (59% body weight) connecting the cervical spine to the thoracic region. For an individual who weighs 770 N (approximately 70kg), force in the neck varies from 98 N. The compressive force gradually increases from the head to the thoracic spine. Shear forces are very small compared with only 4% body weight. The IVD during flexion and extension has deformation values that vary from 25% to 75% of the initial height. The young modulus of the natural disc can vary from 1.7 to 3.4 MPa. Of course, each spine is unique to each person which changes biomechanical properties for everyone [12].

Table 1. Range of movement during the flexion and extension of the cervical spine in different studies [12]

Segment	**Mean range and standard deviation of motion (˚)**			
	Aho *et al*.	Bhalla *et al*.	Lind *et al*.	Dvorak *et al*.
C2-3	12 (5)	9 (1)	10 (4)	10 (3)
C3-4	15 (7)	15 (2)	14 (6)	15 (3)
C4-5	22 (4)	23 (1)	16 (6)	19 (4)
C5-6	28 (4)	19 (1)	15 (8)	20 (4)
C6-7	15 (4)	18 (3)	11 (7)	19 (4)

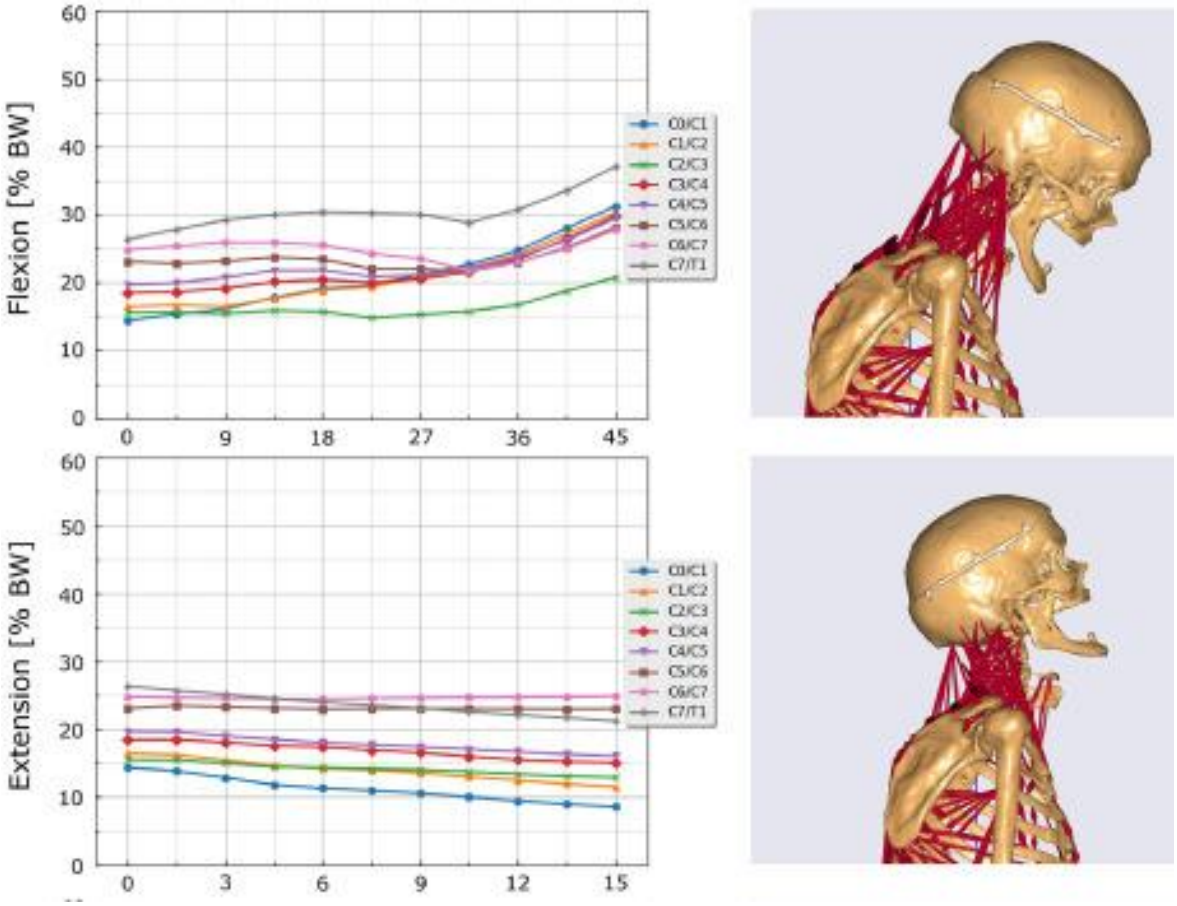

Figure 1.5 Compressive force in the cervical spine as function of neck inclination [12].

1.3. Pathologies of the cervical spine and current treatments

Spinal pathologies such as degenerative disc disease (DDD) and traumatic disc herniation are two of the most common in the world. Due to an injury or trauma, the IVD can lose its integrity causing pain and loss of flexibility. Furthermore, with just normal aging, the spinal discs can lose their hydration and height, causing a loss in back mobility, especially in elders. DDD is one of the leading causes of occupational morbidity. Disc herniation is estimated to be present in 5.5 out of 100,000 people, with 26% needing surgical treatment. [13]

Several solutions can be employed to solve the change in shape or loss of function of the deformed disc. Chirurgical interventions are necessary when therapeutic methods fail, or radiographic imaging indicates nerve compression/damage. These procedures usually start with an anterior discectomy

which is the removal of disc material that compresses the neural elements. Then, there are several methods to restore the IVDs.

Performed in the early 1950s, anterior fusion consists in fusing the vertebrae eliminating the movement of the articulation which can cause degeneration in the adjacent spinal discs. There is still existing debate about the employment of this technique, but the adjacent segment disease remains the major argument against this method [14].

To maintain motion in the articulation and decrease adjacent segment degeneration, the idea of arthroplasty devices started to be described in the 1950s as well [15]. Arthroplasty means “formation of a joint” to relieve pain and restore function. This solution preserves the natural motion by maintaining disc space height and by preserving the natural physiological forces and motion. Spinal arthroplasty procedures include reconstruction or augmentation of the posterior ligaments, insertion of interspinous spacers, replacement, or regeneration of the nucleus pulposus, and total disc replacement (TDR) [16], [17]. These last two methods require the use of an “artificial disc” that tries to mimic the natural structure of the disc, preferably has significant durability, and is easy and safe during implant placement or removal.

This work is aimed at proving the efficiency of prosthetic cervical disc devices by comparing them to natural IVD. The main motivation for this project came from the lack of information about the load-sharing behaviour of the cervical spine since many there are many studies in the lumbar region. Also, almost no other documents compare the prosthetic disc to the natural disc, since there is a lack of basic information about the biomechanics of cervical IVD.

The main objective of this study is to build a biomechanical analysis and comparison between the natural IVD and the artificial prosthetic disc on the cervical spine. By analysing the loads and deformations applied in the vertebrae, the distribution of loads in the cervical spine can be obtained which will allow inferring the advantages and disadvantages of disc arthroplasty devices.

Chapter 2. Disc Arthroplasty Devices

The main purpose of disc arthroplasty devices is the transmission of load and maintenance of motion respecting disc height. The development of these artificial discs has passed through varied iterations and design concepts over the years and some of them provide a satisfying replication of the kinematics of the natural disc. Since there are several design concepts for disc arthroplasty devices, there are also diverse ways of classifying them. As mentioned before artificial discs can be differentiated into two types: the partial disc replacement (PDR) of the nucleus pulposus or total disc replacement (nucleus and annulus). PDR is a less invasive method to cure disc diseases since some structures of the natural disc are kept so it is usually suggested in the initial stages of the degeneration of the disc [18]. TDR devices are more commonly used and have their classification methods for a better understanding of their characteristics and functions.

2.1. Classification of prosthetic discs

Total disc replacement devices can be classified according to their biomechanical properties or range of motion, as constrained, semi-constrained, and non-constrained. Constrained models have mechanical restrictions in their design to allow movement within the natural physiological range, semi-constrained models allow motion inside the physiological range, and non-constrained discs are not restricted in their motion which allows hypermobility. This classification is applied to the different modes of motion of the disc. For example, an artificial disc can be classified as unconstrained in the axial rotation because it does not provide restrictions in rotation but at the same time is also classified as semi-constrained for flexion, extension, and lateral bending because the device allows normal physiological movement. The natural IVD and its surrounding structures can be classified as a semi-constrained system that allows motion in the physiological range and restraints excessive pathologic motion. These devices can also be classified according to the material of the articulating surfaces as metal-on-metal or

metal-on-plastic and according to their anchorage to the vertebrae as stem, screw, or macro-texture [16], [19].

Currently, there are several arthroplasty devices in investigational studies. In Table 2, four of the most studied prostheses that are currently used are shown along with the results of clinical trials [19]. The devices were shown to represent current models that are being used in patients with an array of different classifications. The first two are metal-on-plastic devices. The SB Charité III (DePuy Spine) and the ProDisc (Synthes Inc.) consist of a three-piece design: two cobalt-chrome alloy endplates, with an unconstrained, polyethylene sliding core and with different fixation techniques on the endplates [20]–[22]. The other two prostheses have metal-on-metal bearing surfaces. The Maverick™ (Medtronic) and FlexiCore (Stryker Spine) are artificial discs with a cobalt-chrome two-piece metal-on-metal design with different fixations and a constrained ball-and-socket design [23], [24].

As seen in the different studies analysed in Table 2, there is no device classification comparatively superior or inferior to the other. Each implant and each clinical situation should be evaluated independently to figure out which type of device is best for the desired use. This classification system was mainly created to allow health professionals to better understand the difference between arthroplasty devices. These criteria should help decide which prostheses are adequate for each patient and not judge and assume which group of devices are the best and worst based on the clinical outcomes.

Table 2. Examples of published studies with currently used TDR devices

Arthroplasty devices	**SB Charité III (DePuy Spine)**	**ProDisc (Synthes Inc.)**	**The Maverick™ (Medtronic)**	**FlexiCore (Stryker Spine)**
Classification	Metal-on-plastic Unconstrained for axial rotation, semi-constrained for flexion, extension, and lateral bending	Metal-on-plastic Unconstrained for axial rotation, semi-constrained for flexion, extension, and lateral bending	Metal-on-metal Unconstrained for axial rotation, semi-constrained for flexion, extension and lateral bending, constrained in axial rotation	Metal-on-metal Semi-constrained for flexion, extension and axial rotation Constrained in axial compression
Study	Lu, Sb., Hai, Y., Kong, C. *et al*. [21]	Marnay T. *et al.* [22]	Plais N, Thevenot X, Cogniet A, Rigal J, Le Huec JC. *et al* [23]	Sasso, Rick C., *et al*. [24]
Methods	35 patients indicated for TDR	58 patients underwent TDR	87 patients underwent TDR and 61 were at the final follow up	44 patients indicated for TDR
Follow up time	11.8 years	8-10 years	10 years	2 years
Overall results	87.5% had a successful outcome. 2 patients with adjacent segment degeneration. The study does not evidence the fear of reoperation or late complications.	78% reported good to excellent results without device-related issues. One and two-level implantations showed no difference	Mobility of the prosthesis was preserved in 76.8% of the cases. Back pain decreased and substantial clinical benefit was reached for 55.6%	Compared to fusion, TDR with FlexiCore showed an improved motion range and operative time. It is considered a favourable treatment to DDD over fusion.

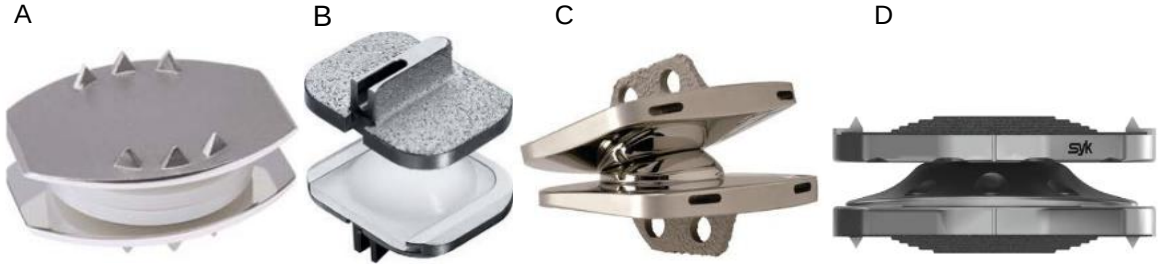

Figure 2.1 A- SB Charité III (DePuy Spine). B- ProDisc (Synthes Inc.). C- The Maverick™ (Medtronic) D-FlexiCore (Stryker Spine) [25]–[28].

2.2. Biomaterials in spinal protheses

Arthroplasty devices must be made of materials capable of resisting natural forces that the human spine creates on discs without breaking or deforming with continued use. These biomaterials must of course be biocompatible and should withstand 30 to 50 million cycles which correspond approximately to 30 to 50 years [29]. Some of the most used materials include:

- Metals and alloys such as:
  - Stainless steel alloys
  - Titanium and titanium alloys
  - Cobalt alloys
- Ceramics, more resistant to wear but more fragile due to their low ductility
- High molecular weight polyethylene, such as UHMWPE (ultrahigh molecular weight polyethylene) or PEEK (Polyether ether ketone) for the nucleus between the metal plates.

These materials are often coated with other biomaterials to promote the implant osseointegration maintaining it stable in the correct position. Coatings can be made with hydroxyapatite, tricalcium phosphate, porous titanium, or chromium-cobalt [29].

The main advantage of using an all-metal artificial disc is the inherent high fatigue strength which should make these discs the longest longevity. On the other hand, the use of non-metallic materials doesn't have the same longevity but can more accurately reproduce the natural disc biomechanics. Polymers and elastomers have a lower modulus of elasticity than metals which makes it easier to replicate native disc dynamics and they can easily absorb the impact energy in the spine [29], [30].

To combine the advantages of both non-metallic and metallic materials, the design of the artificial disc has evolved into a metal-polymer-metal sandwich design. On the extremities of the device, the metallic components provide support and fixation, while the nucleus provides flexibility [30].

2.3. Design concepts in cervical disc arthroplasty devices

2.3.1. Design of the implant

Prostheses for TDR have the main objective of restoring motion stiffness and stability. Several designs have been developed over the years and each one has different outcomes when used. According to design differences, the TDR devices can be divided into two categories with different sub-groups:

- Total disc prosthesis for motion
- Total disc prosthesis for motion and shock absorption
    - Springs
    - Fluid-filled cavity
    - Fibre-reinforced composite
    - Elastomeric polymer

Total disc prosthesis for motion

In this category, the common design concept used for the implant is the “ball-and-socket” gliding interface. As mentioned before in the classification section, the motion of the device can be unconstrained, semi-constrained, and constrained. Some models have a single-gliding interface and others have double-gliding interfaces [31].

However, implants in this category can cause adverse effects on the facet joints and adjacent segments because of the exaggerated motion patterns and lack of shock attenuation.

Total disc prosthesis for motion and shock absorption

To add shock absorption to the previous implants, several design concepts provide favourable mechanical characteristics. Fluid-filled cavities, springs, fibre-reinforced composites, and elastomeric polymers can be combined with the ball/socket gliding interface and other designs to achieve the best disc.

Springs

Springs are combined with other components in the design process because they behave in an uncontrolled manner, and it is necessary to restrain their movement.

An artificial disc designed by Hedman *et al*. contains springs between two metal endplates and has a posteriorly located hinge joint for flexion and extension and control of rotation. This component is not been widely used recently in the design of artificial discs because spring deformations and flimsiness can raise concerns about the device's longevity [32].

Fluid-filled cavity

This type of design choice is often used for PDR and there are some TDR devices with this feature. Usually, the cavity is encased in other two opposing plates and a flexible seal extending between the two plates that provide support and strength [33].

Fibre-reinforced composite structure

TDR devices with a fibre-reinforced composite structure have very similar biomechanical properties to the natural disc.

An artificial disc designed by Kaneda-Abumi consists of a triaxial three-dimensional fabric (3-DF) woven with an ultrahigh molecular weight polyethylene fibre and spray-coated bioactive ceramics on the disc surface. In a study with sheep, the disc was implanted in the lumbar region and after 4 and 6 months the biomechanics and histology were evaluated. The tensile-compressive and torsional properties of the prototype were almost similar to the human lumbar disc. In general, this 3D fabric disc demonstrated excellent in vitro and in vivo performance in biomechanics and interface histology [34].

Elastomeric polymer

As mentioned before, modern designs of the TDR devices are a metal-polymer-metal sandwich layout. The elastomeric polymer layer can be made of silicone, rubber, and polyurethane.

The elastomeric polymer designs by Steffee (Acroflex Disc), made of rubber or silicone, have metal end plates with porous coating for bone in-growth on one plate and a vulcanized polymer core on the other plate. Several compressions and fatigue tests have been conducted. When the implant was tested in compression to 45 kg (frequency of 2 Hz) for 11.5 million cycles in a water bath, the disc was not deformed or chipped in any way [35].

2.3.2. Design concepts for the fixation of the device to the bone

Discs are often coated with other materials to promote osseointegration as referred before. The prosthetic endplates of the artificial discs are often flat or convex to adapt easily to the natural curve of the vertebrae in which they will rest. Surfaces are usually rugged to promote better stability. However, there are other design concepts for the device fixation to the vertebral bone.

Some TDR devices have spikes, cones, fins, or ramps that are perpendicular to the endplates and that penetrate the bone to provide fixation. These protrusions can also have a serrated surface to increase the surface area of contact with the bone.

Some designs also include a screw fixation method. The screws are fixed on the lateral sides of the vertebral bones. Screw fixings on the anterior surface of the vertebral body, in particular for the thoracolumbar spine, present a greater risk due to the vascular system

2.4. The prosthetic Mobi-C cervical disc

The Mobi-C Cervical Disc Prosthesis from Zimmer Biomet was the first cervical disc in the United States approved to treat more than one level of the cervical spine. It is a semi-constrained metal-on-plastic prosthetic disc for flexion, extension, rotation, and lateral bending. It is composed of two metallic endplates and a polymeric core that interlock with each other. The endplates have keels to facilitate fixation to the vertebral body and avoid movement when placed. Mobi-C was determined by the FDA to be statistically superior to fusion at 7 years for two-level cervical disc replacement, based on the primary study endpoint of a prospective, concurrently controlled, and randomized, multi-centre clinical trial. At 10 years, all patient-reported outcomes were equivalent to or improved from 7 years. The Mobi-C Cervical Disc Prosthesis is indicated in skeletally mature patients for reconstruction of the disc from C3 to C7 following discectomy at one or two contiguous levels [36]–[38].

This device was chosen for this project to represent the prosthetic model in the experimental methods and to be compared to the native disc since it has been clinically used and approved to restore motion in the cervical spine.

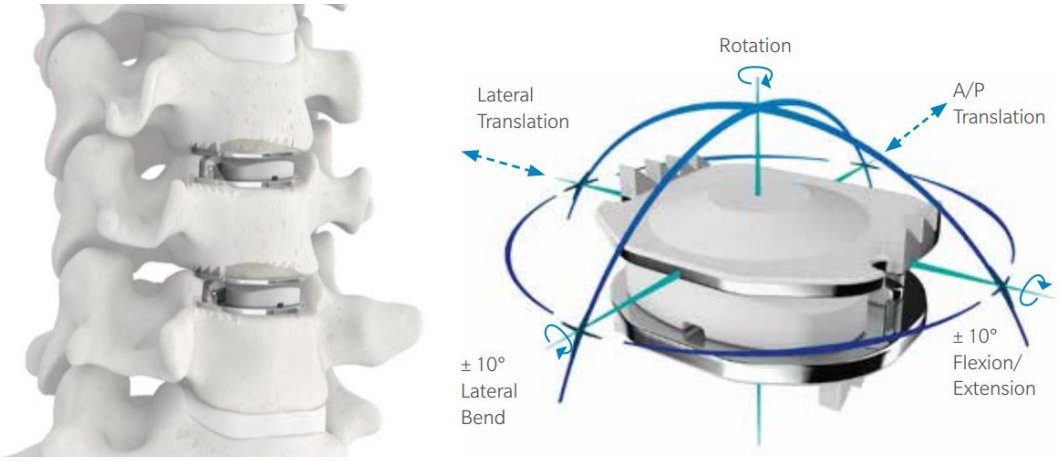

Figure 2.2 The Mobi-C prosthetic disc by Zimmer Biomet [38], [39].

2.5. Operative Procedure

Generally, TDR devices involve an anterior retroperitoneal approach for exposing the anterior disc space. The patient is positioned in a neutral position on a radiolucent operating table. A total discectomy is the first procedure that involves removing the damaged disc. The lateral annulus is preserved on both sides. Disc removal is performed using specialized tools like curettes for scraping away biological tissue or debris and gouges to hollow out the bone. It is important to carefully remove the cartilaginous end plates while preserving the bony endplates to minimize the risk of implant subsidence. The artificial disc is placed using an individualized combination of sizing, trialling, midline verification, and disc placement [40]. In figure 2.3, the Mobi-C surgical approach can be seen along with the pre-assembled PEEK cartridge insertion tool.

Figure 2.3 Mobi-C surgical approach [38].

2.6. Device stability and wear

Prolonged use is the main focus when total disc arthroplasty is advised to the patient. The implant should be able to stay in the designated position without fracturing, deforming, or moving for the longest time possible without surgical intervention. However, with the constant stress and motion of the devices, it is vital to choose the right materials and design concepts.

Implant wear is associated with biomechanical issues such as subsidence, migration, under-sizing, and adjacent fusion. Devices with a more constrained motion may be advantageous because they protect the surrounding structures from overloading. If there is the formation of wear debris, these will slowly wear off parts of the artificial disc, leading to its degradation over time. Some discs have a thin membrane that surrounds the entire disc to trap any wear debris, preventing them from being dispersed into the body tissues and fluids [41].

As shown in this chapter, disc arthroplasty devices can vary significantly in terms of classification, design, and biomaterial. As seen in several studies, some designs can be more adequate for some patients while others might not. The choice of the correct model of the implant is an individual process that should be tailored to each patient and their need.

2.7. Previous studies about the native and prosthetic cervical disc

This project is aimed at biomechanically comparing the native and prosthetic cervical disc, mainly, their load sharing mechanisms. The forces applied in the cervical spine are distributed between relevant anatomical components and include compressive forces, shear forces and bending moments. In this work, the main focus is the compressive forces applied to the vertebral body. But first, it is important to mention previous studies about the native and the prosthetic cervical disc.

Many studies have clarified load-sharing or isolated component loads in the lumbar region of the spine. In this region, pressure sensors have been used to analyse IVD biomechanics, strain gauges have been used to measure loads in the cervical spine [42], [43] . However, in the cervical region of the spine there is scarce experimental data on disc pressure behaviour. There are also very few studies. which have focused on load sharing in the cervical spine and even less comparing native and prosthetic discs. This may be due to the size of cervical discs which are small compared to their counterparts in the lumbar and thoracic spine.

Cripton *et al*. studied the load sharing mechanisms under non-destructive compression loading in the native cervical disc. Cadaveric spinal units were used with an IVD pressure sensor and with tri-axial strain rosettes on the vertebral body anteriorly and at the lateral masses posteriorly. The vertebral body rosettes exhibited an increase in compressive strain with increasing flexion posture and a decrease in compressive strain with increasing extension angles. The results suggest that the anterior column (vertebral body and IVD) of the cervical spine transmits the bulk of the applied compressive forces at all flexion and extension postures. This is why this project focuses mainly on loads in the vertebral body [44].

McNally *et al*. developed a technique for measuring the distribution of stress within loaded cadaveric IVDs. A strain-gauged membrane was mounted on the side of a needle inserted in the disc to provide vertical and horizontal components of compressive stress. The results showed that mechanical behaviour of individual disc tissues are dependent on their location and their loading as well. In figure 2.4 the stress profiles of the disc are shown for a compressive force of 2000 N at a neutral position. In the central region of the disc (“functional nucleus”), components

of stress are approximately constant and equal indicating the region behaves as a liquid. For the posterior region of the disc (“functional posterior annulus”), compressive stresses are higher than in the anterior region of the disc (“functional anterior annulus”). This shows that the anterior region of the IVD is predominantly in tension while the posterior region offers higher resistance to the compressive load. Because stress profiles vary so much with age and degeneration, it is not possible to generalize the results for everyone but, the data obtained shows the IVDs behave like a collection of fluid compartments that have unique biomechanical properties that vary with load and loading history [43]

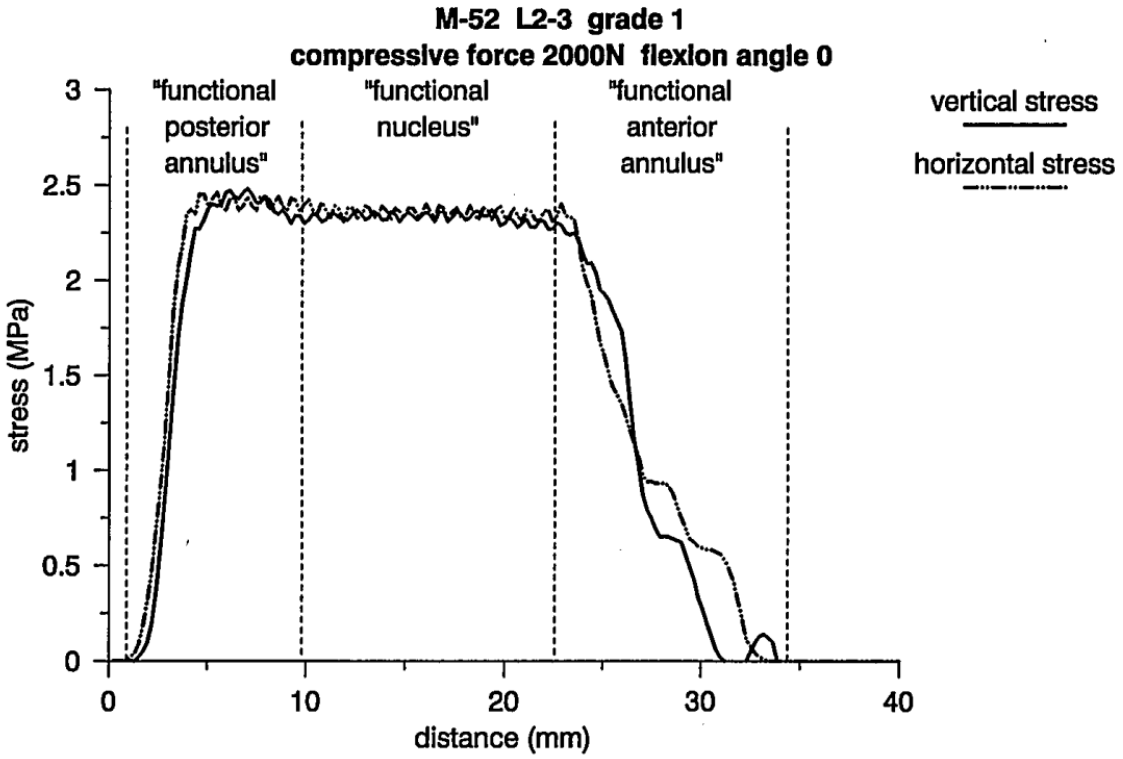

Figure 2.4 Typical pair of anteroposterior stress profiles in IVDs [43].

Bonnheim *et al* investigated the role of size and stiffness of TDR implants on load-transfer within a vertebral body. Using data from a micro-computed tomography scan, generically shaped total disc arthroplasty implants were virtually implanted on a human lumbar vertebral body and analysed using parametric micro-computed tomography-based finite element analysis in compression and flexion-induced impingement. Two load cases were tested: 800 N in uniform compression and flexion-induced anterior impingement. Results were compared to those of an

intact model without an implant. The results show that TDR implants increased stress in the bone tissue by over 50% in substantial portions of the vertebra (figure 2.5). These changes depended more on implant size than material, and there was an effect between implant size and loading condition. It was concluded that most TDR implants, regardless of their overall stiffness properties, will diminish the load-bearing role of the cortical shell in compression, rely more on anterior trabecular regions and the anterior cortex to resist the loads that develop in flexion, and also re-distribute stress in a larger portion of the underlying vertebral body [45].

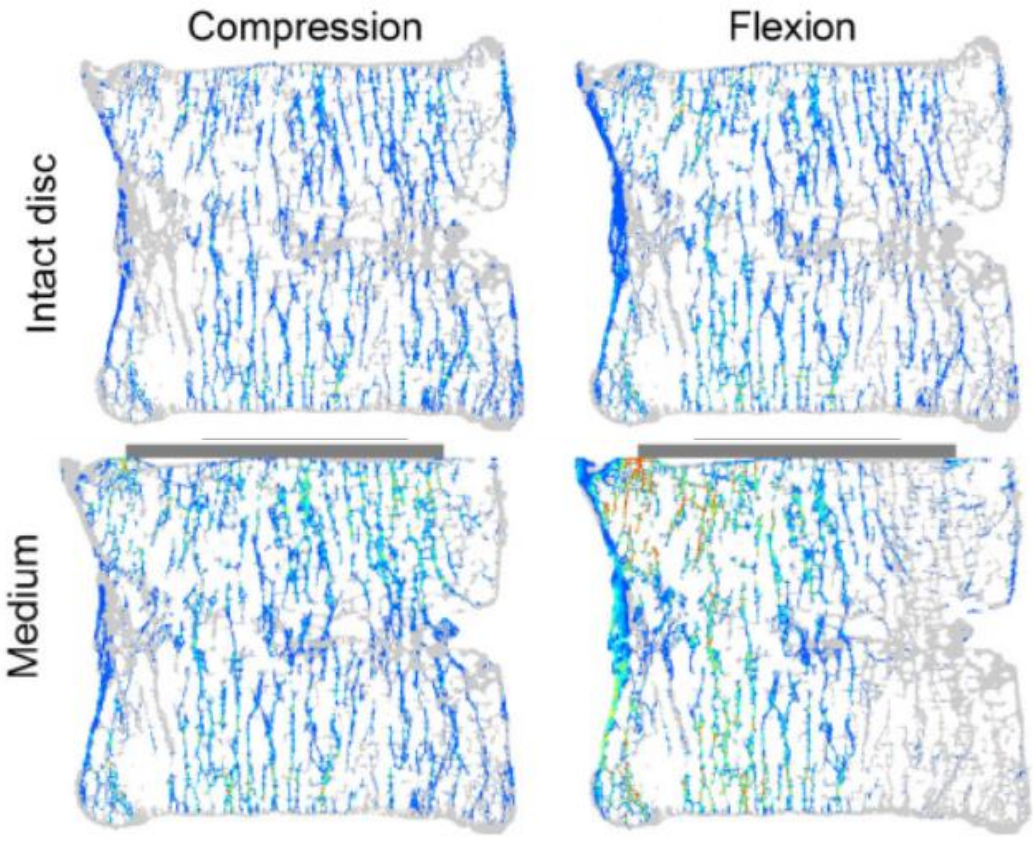

Figure 2.5 Minimum principal stress (MPa) in the bone tissue at amid-sagittal cross-section (0.5 mm thick) for the intact disc and medium metallic implant model in compression and flexion. Adapted from [45].

Chapter 3. Materials and Methods

In this chapter, the experimental procedures done in this work are described. An experimental model was created to mimic the cervical spine in a tensile tester machine. The C5 and C6 vertebrae were chosen for this study because they are similar in structure, and they are located in the lower part of the cervical spine where loads applied are higher. This makes it easier to compare the natural disc with the prosthetic one and showcases the high loads that a disc and prostheses can resist. It is described in this chapter how the experimental model was made along with how the deformation of the natural and prosthetic disc was measured for different positions of the cervical spine.

3.1. Materials and experimental assembly of the C5-C6 segment

The main aim of this model was to approximately replicate the load present in the real cervical spine, mainly in the disc between the C5 and C6 vertebrae. The experimental model consists of two vertebrae that will surround the disc, along with two connected pieces on each side that support and connect the vertebrae to the tensile tester machine.

3.1.1. The C5 and C6 vertebrae

The vertebrae used are foam cortical shell models, made of a rigid foam shell with inner cancellous material developed by Sawbones Europe AB (figure 3.1) [46]. To resemble trabecular bone the vertebrae were painted and completed with an outer shell of epoxy resin to better mimic the mechanical properties of the bone. The C5 and C6 vertebrae were fixed to the upper and lower support pieces respectively with epoxy resin.

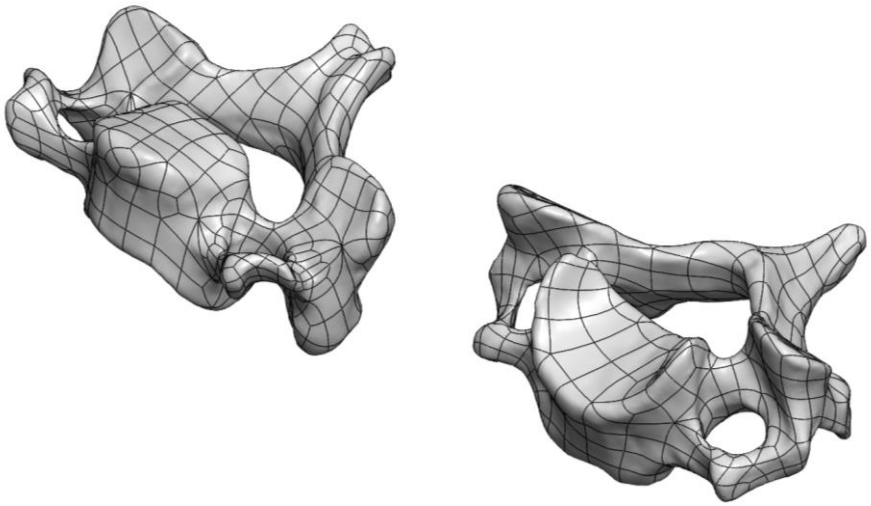

Figure 3.1 3D models of the C5 (left) and C6 (right) vertebrae by Sawbones Europe AB.

3.1.2. Natural disc model

To recreate a natural IVD, a 3D model was created using the SolidWorks 2021 design program (figure 3.2). It was designed to ensure a perfect contact surface between the vertebral endplates and the disc. This model was then fabricated using an industrial 3D printing process called PolyJet. This process builds prototypes with flexible mould rubber materials and different hardness values. The PolyJet procedure begins by spraying small droplets of liquid photopolymers in layers that are instantly UV cured. Voxels (three-dimensional pixels) are strategically placed during the build, which allow for the combination of both flexible and rigid photopolymers. The fine layers of materials accumulate on the build platform to create accurate 3D-printed parts. Each PolyJet part is completely coated in support material during the build, which later is removed by hand using a pressurized water stream and a chemical solution bath. No post-curing is required after the manufacturing process [47]. Three discs were manufactured with three different hardness values: 1 MPa, 1.35 MPa, and 2.15 MPa. Anteroposterior disc length is approximately 17 mm, lateral distance is 18 mm and disc height is 5.5 mm.

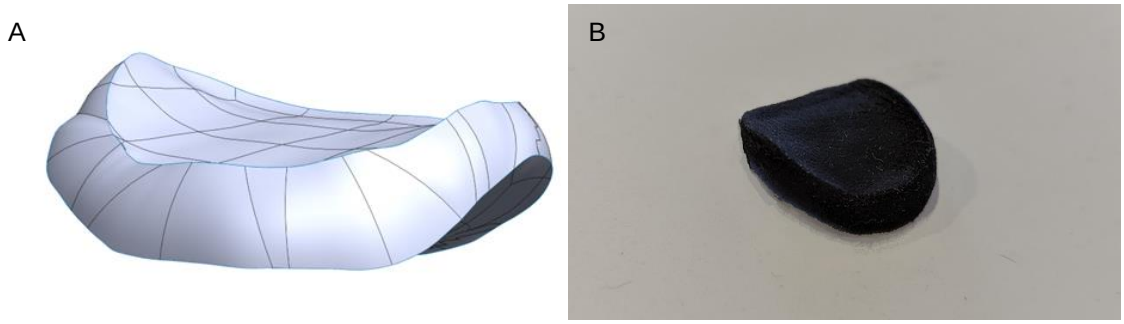

Figure 3.2 A- 3D model of the natural IVD. B- 3D printed Polyject disc

To compare the natural disc with the prosthetic disc, only one model with the highest hardness value was chosen (2.15 MPa) since it has the most approximate value of hardness to the native disc of a human [12].

3.1.3. Prosthetic disc model

The Mobi-C cervical disc retrieved from a patient who previously used this prosthesis was used in this work (figure 3.3). In this model, anteroposterior disc distance is 15 mm on the endplates, lateral distance is 17 mm and disc height is 6mm. As mentioned before it is composed of two metallic endplates with a polymeric interior. It allows all the movements of the normal cervical spine and it has similar biomechanical properties to the natural disc.

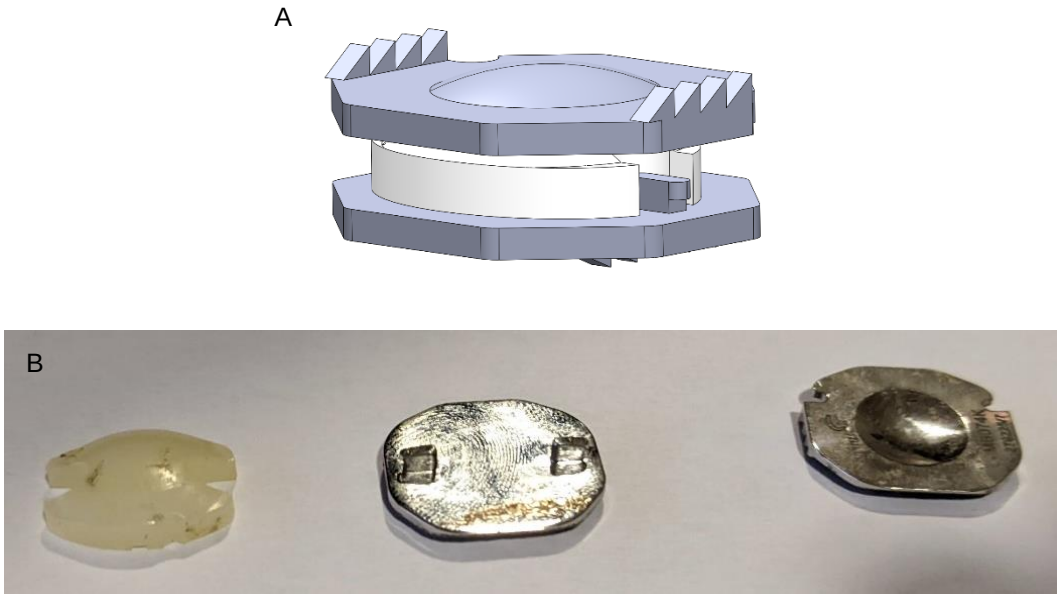

Figure 3.3 A- 3D model of Mobi-C prosthetic disc. B- Mobi-C disc implant used

3.1.4. Support pieces

The support pieces of the assembly permit restricted movement of the vertebrae which will allow simulating flexion and extension of the cervical spine. They connect the vertebrae to the tensile test machine and interlock using pins in different holes. Three positions were tested with the experimental model: neutral position (zero degrees), flexion of 10 degrees, and extension of 10 degrees as shown in figure 3.4.

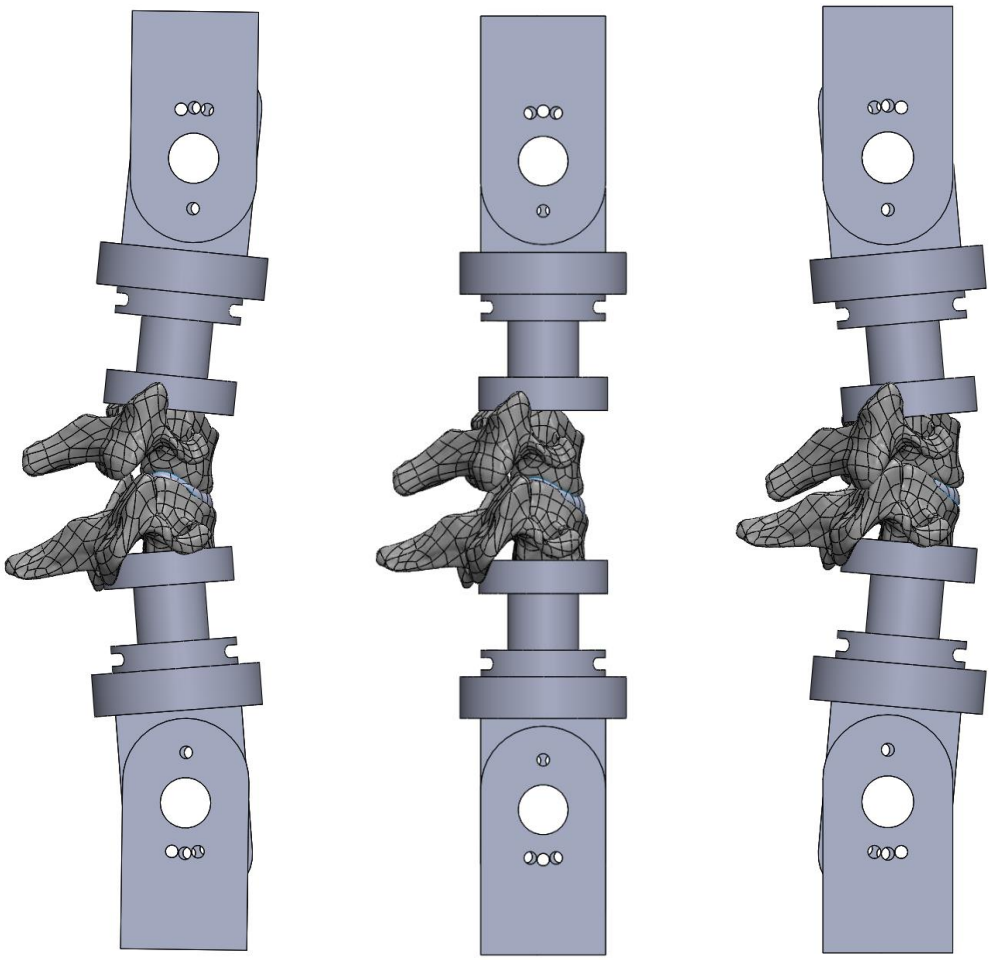

Figure 3.4 Support pieces providing restricted movement to the assembly like flexion of 10˚(left), 0˚ (middle) and extension of 10˚(right).

3.1.5. Ligaments

Ligaments were taken into account by fixing elastic bands to the support pieces in the anterior and posterior positions. Since there was a lack of space and fixation methods for the elastic bands, it was only possible to use three elastic bands in the anterior part of the model which corresponds to the anterior longitudinal

ligament, and three elastic bands in the posterior position which mainly correspond to the posterior longitudinal ligament. The six elastic bands were tested in the tensile tester machine to see their stiffness value in the elastic deformation region as seen in figure 3.5. The initial deformation or neutral position (0 N) of the bands was 180 mm. In total, the six elastic bands put in the system correspond to a stiffness of approximately 1 N/mm. Of course, the elastic bands do not represent a replica of the native ligaments in the cervical spine in terms of stiffness and force that they exert and also the position they are in.

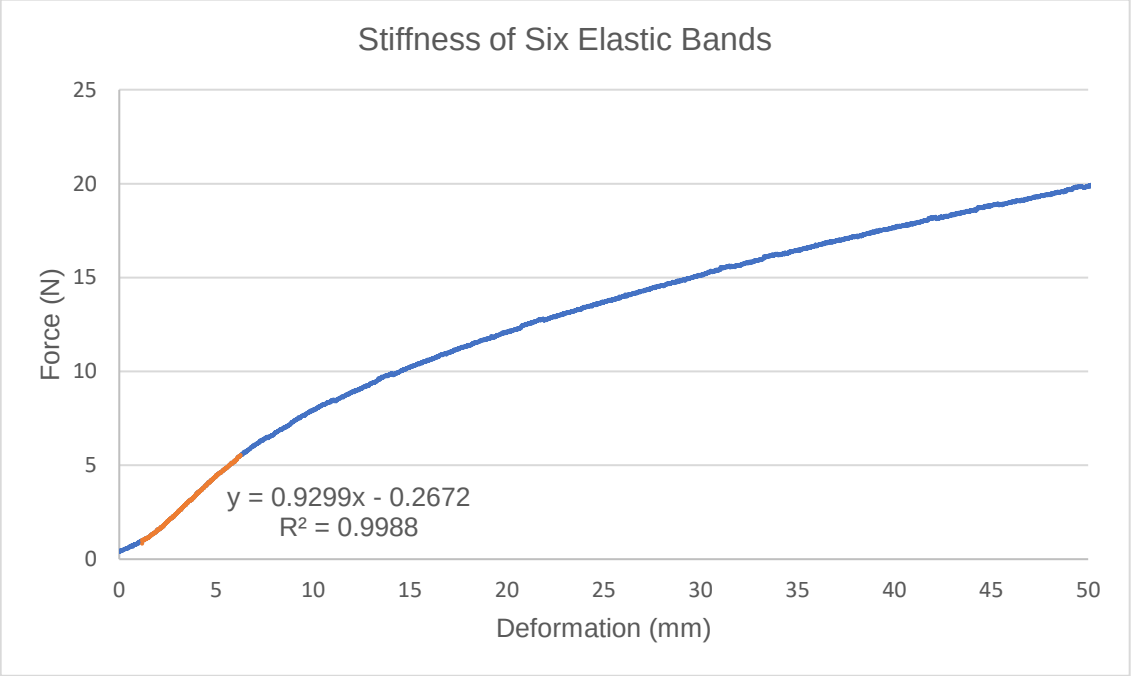

Figure 3.5 Graph of force versus deformation for six elastic bands.

3.1.6. Instrumentation

To measure the deformation on each vertebra, four strain gauges were used. A strain gauge is a transducer capable of measuring deformations on the surface attached to it, which in this case is the cortical surface of the vertebra (epoxy resin covering the foam models). These sensors shrink and extend due to applied forces which cause their electrical resistance to change proportionally and allow the measurement of deformation. Tri-axial strain gauges ((KFG-1-120-D17-11L3M2S, Kyowa Electronic Instruments Co, Ltd, Tokyo, Japan) were chosen to measure strain in the anterior and posterior centre of the vertebral body of C5 and C6. The tri-axial strain gauges contain three filaments aligned at a 45˚ angle to each other

which allows the analysis of the vertical (sagittal) force as well as diagonal loads on the cervical spine (figure 3.6A). Each strain gauge was tested after being fixed to the vertebrae with a multimeter to check the internal resistance of 120 Ω.

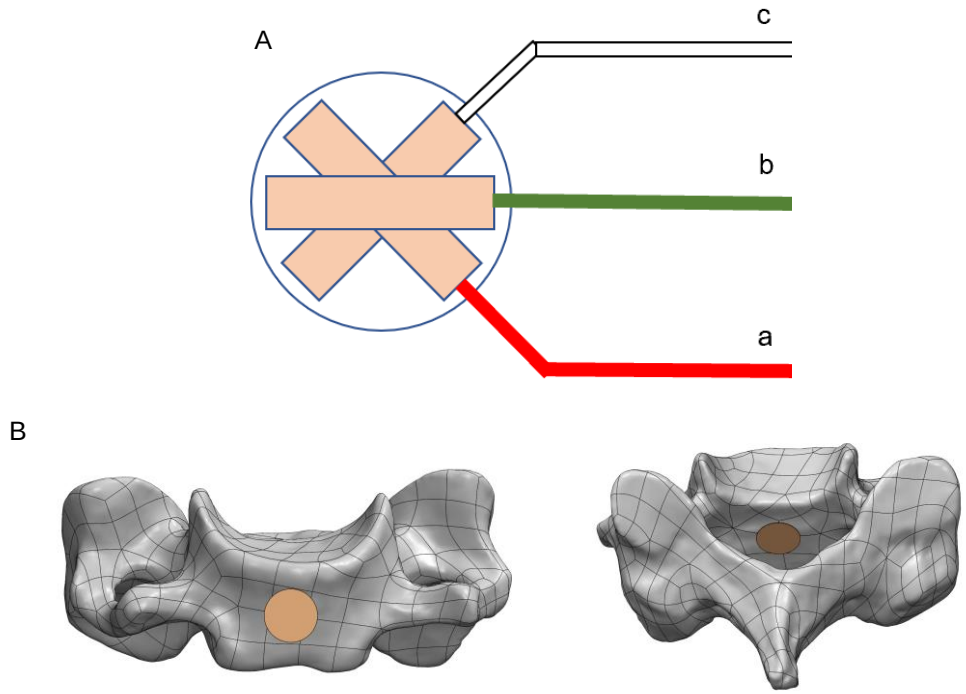

Figure 3.6 A - Representation of the strain gauges filaments and corresponding letters. B- Approximate position of the strain gauges in the anterior and posterior facets of the vertebral body on C5 and C6.

In this work, the maximum and minimum principal strains ($\boldsymbol{\varepsilon_{max}}$ and $\boldsymbol{\varepsilon_{min}}$) were the main variables assessed. Since most of the force applied in the cervical spine is made in the vertebral body of each vertebra, the four sensors were fixed to the anterior and posterior facets of the two vertebrae approximately in the centre (sagittal plane) as seen in figure 3.6B. This will allow measuring the distribution in loads that pass through the IVD for each position. For each of the four positions where strain gauges were placed, the principal strains were calculated using each filament of the sensors ($\boldsymbol{\varepsilon_a}$, $\boldsymbol{\varepsilon_b}$ and $\boldsymbol{\varepsilon_c}$). Each filament registered different values during compression and decompression of the experimental model and with equations 3.1 and 3.2, the maximum and minimum principal strains were calculated:

$$\boldsymbol{\varepsilon_{max}} = \frac{\mathbf{1}}{\mathbf{2}} \left[\boldsymbol{\varepsilon_a} + \boldsymbol{\varepsilon_c} + \sqrt{\mathbf{2}\left[(\boldsymbol{\varepsilon_a} - \boldsymbol{\varepsilon_b})^{\mathbf{2}} + (\boldsymbol{\varepsilon_b} - \boldsymbol{\varepsilon_c})^{\mathbf{2}}\right]}\right] \quad (3.1)$$

$$\boldsymbol{\varepsilon_{min}} = \frac{\mathbf{1}}{\mathbf{2}} \left[\boldsymbol{\varepsilon_a} + \boldsymbol{\varepsilon_c} - \sqrt{\mathbf{2}\left[(\boldsymbol{\varepsilon_a} - \boldsymbol{\varepsilon_b})^{\mathbf{2}} + (\boldsymbol{\varepsilon_b} - \boldsymbol{\varepsilon_c})^{\mathbf{2}}\right]}\right] \quad (3.2)$$

3.2. Experimental studies with the natural disc

All the components were assembled carefully and connected to the tensile tester (Autograph AGS-X Series 10 kN). The first tests were conducted with the natural disc placed between the vertebrae. The whole assembled experiment can be seen in figure 3.7.

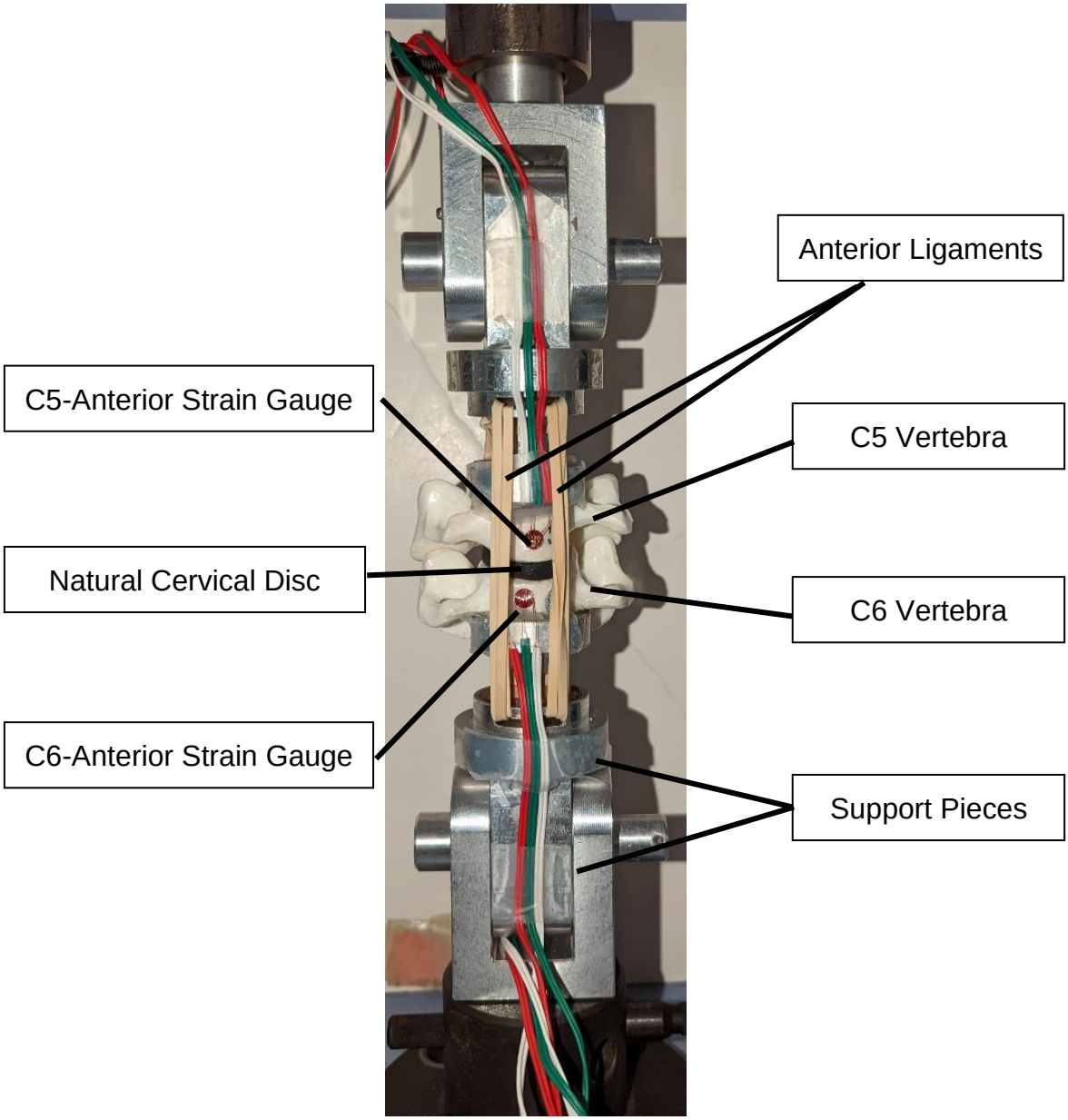

Figure 3.7 – Experimental assembly with the natural IVD.

The tensile tests conducted followed the same pattern for all the scenarios in this work (flexion, neutral, extension, with prostheses or with natural disc). They started with a neutral force, which means the only force applied to the vertebrae and the disc was the one applied by the elastic bands which was measured at approximately 10 N. Then the machine applied vertical force over time with a velocity of 0.9 N/s until a decided maximum of 50 N which corresponds only to the weight of the average head of a human (5 kg). After 20 seconds with the maximum load applied, the force was decreased until it reached the initial load (figure 3.8). Five cycles of this procedure were made for each of the tests to ensure precision and repeatability of the results. Results were extracted with a computer from the four strain gauges and saved for analysis. The final three cycles were the ones analysed because the first two cycles usually have irregularities due to adjustments and stabilization of the disc in its position on the vertebral body. Using the final three cycles of the strain data from the sensors ensures precise and accurate information on the deformation of the vertebrae. The values for $\boldsymbol{\varepsilon_{max}}$ and $\boldsymbol{\varepsilon_{min}}$ for each cycle were calculated and the mean maximum and minimum values were determined.

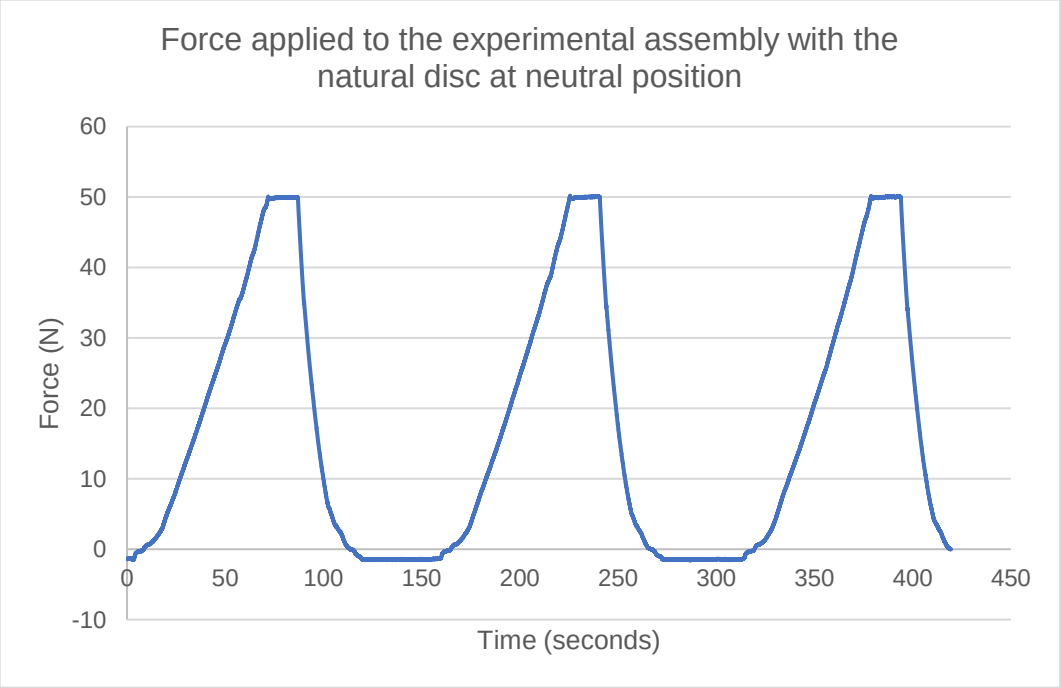

Figure 3.8 – Example of the three tensile cycles conducted for each scenario.

3.2.1 Testing different natural disc hardness values

Since three models of the natural IVD with different hardness values were made, each one was tested with a neutral position of the spine to see their respective deformation in the strain gauges in the vertebrae. Three different hardness values: 1 MPa, 1.35 MPa, and 2.15 MPa give different $\boldsymbol{\varepsilon_{max}}$ and $\boldsymbol{\varepsilon_{min}}$ results which were saved and analised. As mentioned before, to compare the natural disc with the prosthetic disc, the model with the highest hardness value was chosen (2.15 MPa) since it has the most approximate value of hardness to the native disc of a human.

3.2.2. Measuring strain values for different positions of the spine

With the natural disc (2.15 MPa) in position between the vertebrae, strain values on the four sensors were obtained for three different positions of the cervical spine: extension of 10 degrees, neutral position and, flexion of 10 degrees. These results allow to calculate $\boldsymbol{\varepsilon_{max}}$ and $\boldsymbol{\varepsilon_{min}}$ which will be later compared to the results with the prosthetic disc.

3.3 Experimental studies with the prosthetic disc

The Mobi-C prosthetic disc was inserted in the experimental assembly in place of the natural disc. To increase the area of contact of the vertebral body with the prosthesis, the top of the C6 and the bottom of the C5 vertebral body had to be scraped with a file before insertion. This allowed the prosthetic disc to be firmly placed between the vertebrae without significant movement. It is important to note that there was still a minor gap between the disc and the surface of the vertebral body which will make the load transmitted by the disc not completely uniform. The assembly with the prosthetic disc can be seen in figure 3.9.

Figure 3.9 Experimental assembly with the prosthetic disc placed between the vertebrae.

Strain values of the four sensors in the assembly were obtained for three positions of the spine: flexion, neutral and extension. $\boldsymbol{\varepsilon_{max}}$ and $\boldsymbol{\varepsilon_{min}}$ were then calculated with this data and compared with the assembly with the natural disc.

Chapter 4. Experimental Results

In this chapter, the experimental results obtained are presented. In the first section, strain results are shown the experimental assembly with the natural disc. Figure 4.1 shows the mean maximum and minimum principal strain values measured by the different strain gauges placed in the C5 and C6 vertebrae for the neutral position with a natural disc. Table 3 and figure 4.2 shows the $\boldsymbol{\varepsilon_{max}}$ and $\boldsymbol{\varepsilon_{min}}$ values for the three different natural discs tested with three different hardness values. In the second section, strain results are shown for the assembly with the prosthetic disc at neutral position (figure 4.3). In the third section table 4 shows a comparison between the highest $\boldsymbol{\varepsilon_{max}}$ and lowest $\boldsymbol{\varepsilon_{min}}$ values for the natural and prosthetic disc. With these results it is shown that values are different for the natural or the prosthetic disc and of course, different positions (neutral, flexion, and extension) also change the deformation seen in different parts of the vertebral body which will be discussed in the next chapter.

It is important to mention that when changing the positions of the experimental models, the starting position of the measurement (force applied is zero) is not the same. For example, when changing position from neutral to flexion of 10 degrees the centre of rotation changes, so the position where the force applied in the vertebral body is different.

4.1. Results for the experimental assembly with the natural disc

As mentioned before, the first cycles of applying force to each position and disc were not used since they usually display abnormal changes in deformation. This is because the disc initially changes position from where it is placed and adapts to the form of the vertebral body. One curve of the last three cycles out of five is shown in figure 4.1.

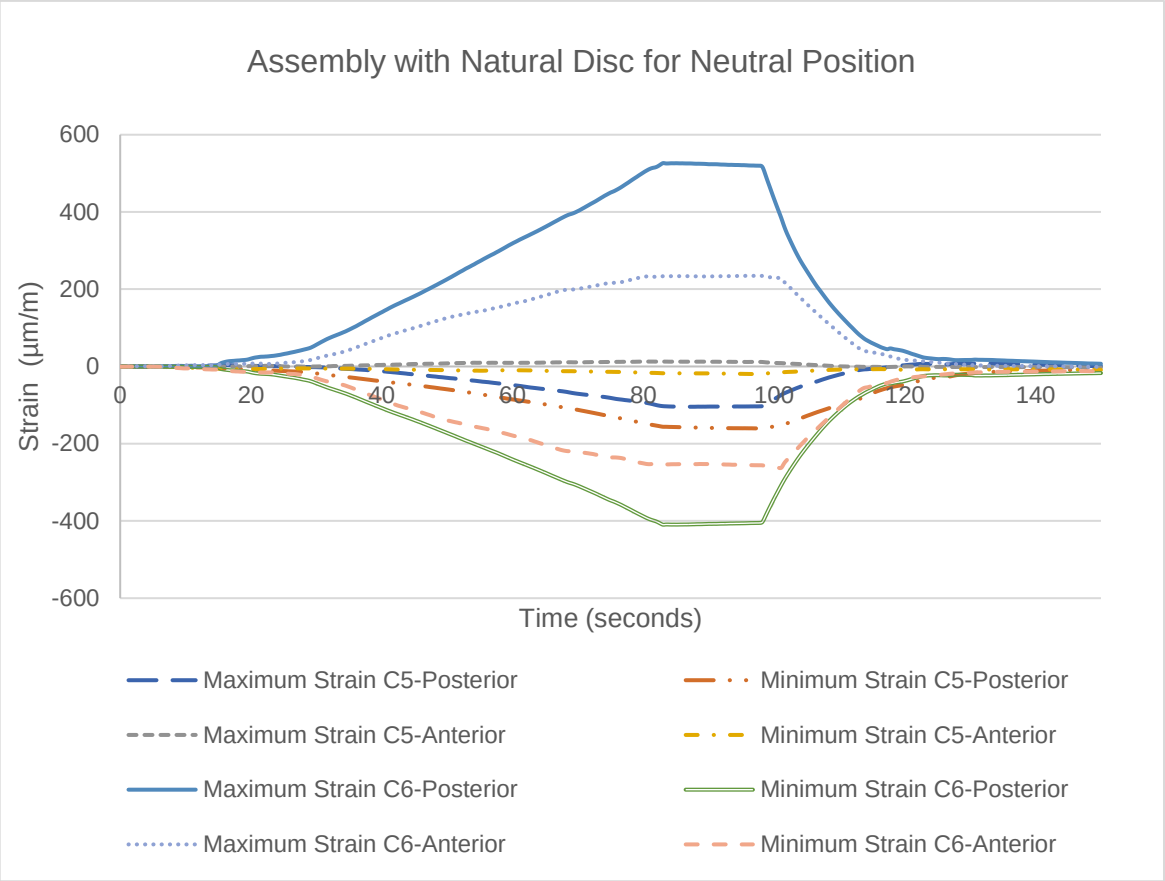

Figure 4.1 Maximum and minimum strain of the vertebrae with the natural disc (2.15 MPa)

Table 3. Mean strain values obtained for three natural discs with different hardness values

		Strain Values ± Standard Deviation (µm/m)		
Natural Disc / Strain Gauge		**1.00 MPa**	**1.35 MPa**	**2.15 MPa**
C5-Posterior	ε_{max}	15.02 ± 2.30	12.93 ± 2.03	26.41 ± 1.87
	ε_{min}	-189.73 ± 3.12	-204.54 ± 2.95	-187.60 ± 2.54
C5-Anterior	ε_{max}	116.05 ± 1.16	108.36 ± 1.58	113.78 ± 2.36
	ε_{min}	-173.85 ± 4.52	-147.74 ± 4.08	-149.61 ± 5.38
C6-Posterior	ε_{max}	404.05 ± 3.94	389.47 ± 2.59	441.73 ± 1.86
	ε_{min}	-385.43 ± 1.52	-378.79 ± 2.03	-431.03 ± 3.52
C6-Anterior	ε_{max}	39.05 ± 5.72	25.23 ± 4.98	62.83 ± 4.53
	ε_{min}	-12.54 ± 6.92	-11.08 ± 5.67	-14.80 ± 4.82

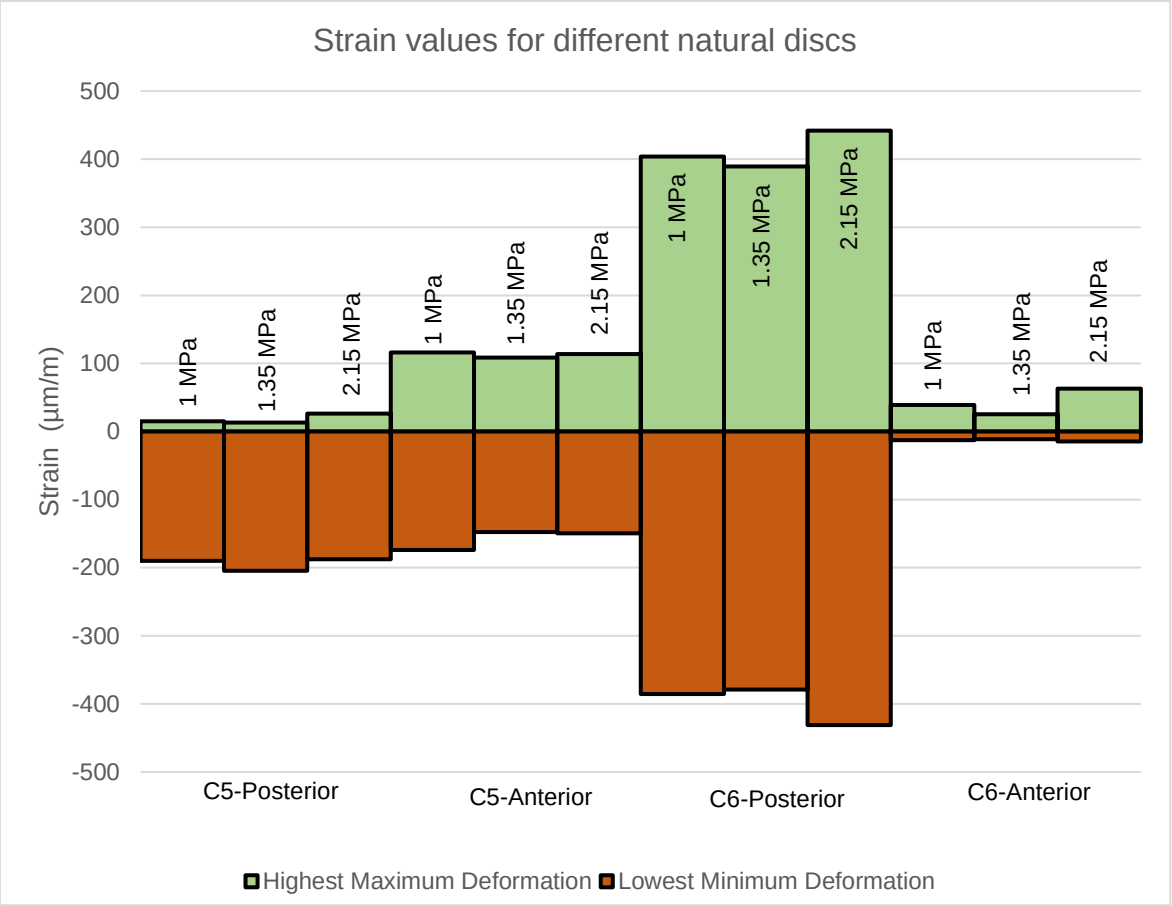

Figure 4.2 Bar graph of strain values for three natural discs with different hardness values.

4.2. Results for the experimental assembly with the prosthetic disc

In the prosthetic disc, the keels on the upper and lower surfaces can dig into the vertebra when force is applied which allows a better fixation. Because of this condition, the results analysed and shown are from the last three cycles of five where there is no apparent sudden change in the disc position which gives more accurate information. From these cycles the mean $\boldsymbol{\varepsilon_{max}}$ and $\boldsymbol{\varepsilon_{min}}$ values were calculated.

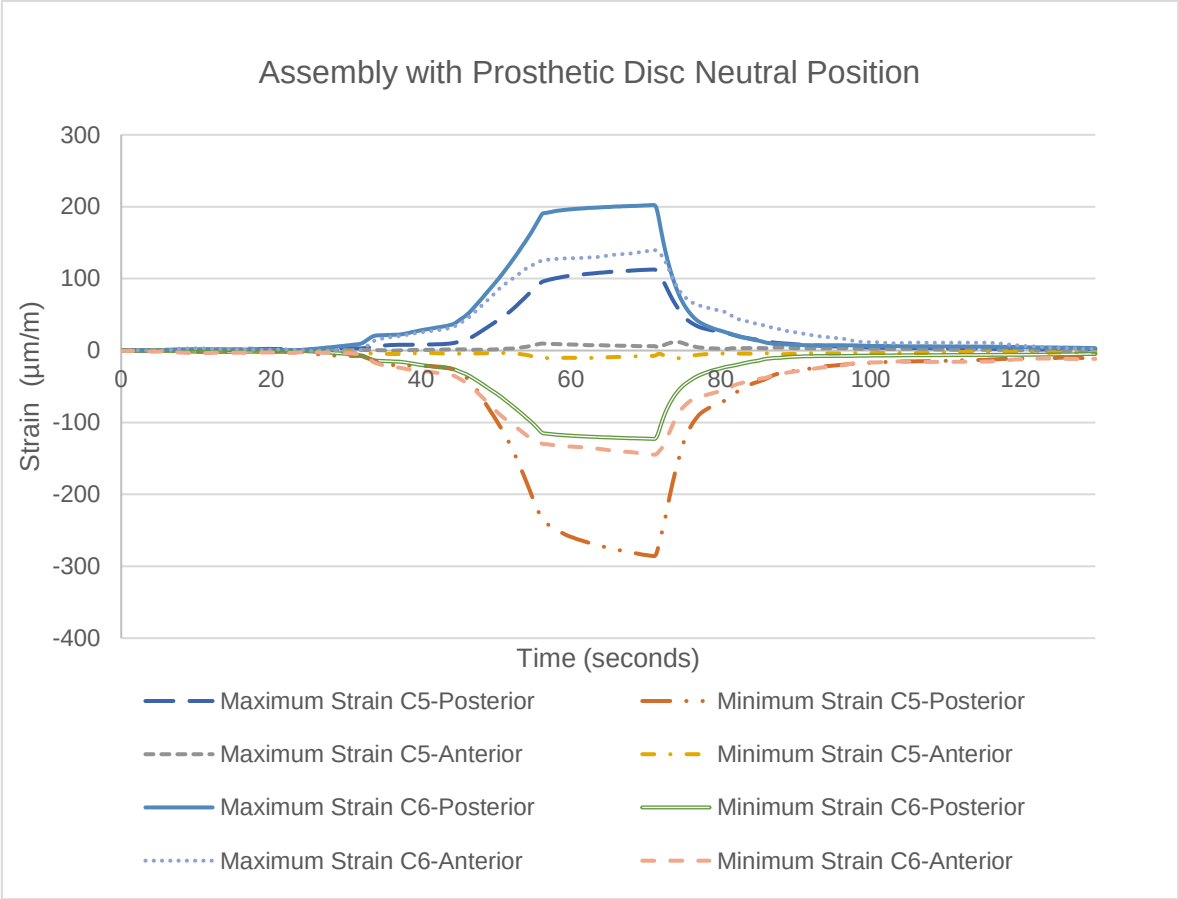

Figure 4.3 Maximum and minimum strain of the vertebrae with the prosthetic disc (2.15 MPa).

4.3. Comparison of natural and prosthetic disc models results

Table 4. Comparison of mean strain values obtained for the natural and prosthetic disc models.

Strain Gauge		**Strain of Natural Disc ± Standard Deviation** (μm/m)			**Strain of Prosthetic Disc ± Standard Deviation** (μm/m)		
		Neutral Position	Flexion 10˚	Extension 10˚	Neutral Position	Flexion 10˚	Extension 10˚
C5-Posterior	ε_{max}	7.91 ± 2.57	11.59 ± 0.91	15.46 ± 1.56	112.64 ± 3.56	37.55 ± 0.88	96.54 ± 6.68
	ε_{min}	-160.51 ± 2.29	-130.11 ± 1.81	-231.00 ± 14.03	-285.84 ± 2.44	-63.15 ± 2.68	-251.14 ± 9.97
C5-Anterior	ε_{max}	12.70 ± 3.11	14.37 ± 8.32	5.64 ± 2.17	11.97 ± 0.52	28.90 ± 7.13	13.43 ± 3.60
	ε_{min}	-19.90 ± 6.88	-105.66 ± 2.09	-8.59 ± 6.97	-11.07 ± 1.06	-22.68 ± 0.73	-14.13 ± 0.96
C6-Posterior	ε_{max}	526.40 ± 4.68	244.72 ± 1.29	504.36 ± 102.37	202.26 ± 0.52	129.06 ± 1.26	219.28 ± 3.70
	ε_{min}	-409.69 ± 1.18	-225.82 ± 2.10	-503.58 ± 91.19	-122.87 ± 1.82	-115.02 ± 1.94	-134.05 ± 2.07
C6-Anterior	ε_{max}	234.84 ± 4.15	273.93 ± 0.01	145.07 ± 26.18	139.57 ± 1.16	115.34 ± 11.84	97.01 ± 2.30
	ε_{min}	-263.09 ± 7.65	-323.59 ± 2.48	-169.05 ± 31.19	-144.84 ± 1.48	-72.88 ± 3.76	-124.50 ± 6.98

Chapter 5. Discussion

This study aimed at analysing and comparing the biomechanical behaviour of the natural and prosthetic discs in the cervical spine by successfully measuring strain in the adjacent vertebrae. The main objectives of this project were accomplished with results that corroborate the behaviour of the real spine.

Of course, the cervical spine is a very complex structure to understand and replicate so several possible errors are associated with the experimental methods. Experimental flaws like disc instability, sensor meddling, unstable support pieces, lack of ligaments, absence of muscle forces and micro changes in the assembly from day to day, cause mistakes in the data retrieved as seen in some results. Also, the natural disc model used with an elastic material did not fully replicate the native disc in the spine because when extending and flexing the neck, the disc naturally should extend to accommodate the gap between the vertebrae which did not happen in this experimental model.

5.1. Strain with the natural disc in the assembly

5.1.1 Different natural disc hardness values

The three natural discs made from an elastic material with three different hardness values caused different values of strain to the adjacent vertebrae as shown in Table 3 and figure 4.2.

For each disc, the highest absolute values for the maximum and minimum principal strains were felt at the C6-Posterior position which means high load values are applied through the disc and in the posterior part of the bottom vertebrae. On the contrary, the lowest absolute values of strain were measured at the anterior part of the C6 vertebra.

Comparing the three discs, the lowest absolute values of $\boldsymbol{\varepsilon_{max}}$ and $\boldsymbol{\varepsilon_{min}}$ were measured for the 1 MPa disc followed closely by the 1.35 MPa disc. The highest absolute value of strain was obtained for the 2.15 MPa disc so the higher the value of hardness in the natural disc, the higher the strain felt in the adjacent vertebrae.

This is theoretically correct because when increasing hardness, the harder it is to elastically deform the disc, so the load applied to the system increases in the vertebral body. So, it can be concluded that, when increasing hardness of the disc, the load of the vertical load passes less through the anterior part of the vertebra (body and IVD) and more trough the posterior part of the cervical spine (articular process and lamina) since the disc deforms less decreasing loads that are transmitted through it.

As mentioned before, the 2.15 MPa was used moving forward since it reflects the most accurate value of hardness to the native cervical disc [12].

5.1.2. Strain with the natural disc for different positions

Looking at figure 4.1, the strain over time represents the behaviour described in chapter 3. It can be observed that there is a gradual increase in strain as force is applied to the system until it reaches 50 N. Then the deformation is maintained and decreased when the force applied goes back to zero, which leads to the initial position and deformation of the assembly. However, different sensors registered different maximum and minimum values of principal strain which change in different positions of the system.

As seen in table 4, in the neutral position of the model, the highest absolute values were measured in the C6-Posterior and below that in the anterior section of the same vertebra. The lowest values were measured in the anterior part of the C5 vertebral body. So, in this assembly, we can deduce that the load applied to the system is mostly transmitted by the posterior section of the vertebral body. This conclusion is in accordance with the results observed in [43]. McNally *et al*. showed that in the central region of the disc, components of stress are approximately constant while for the posterior region of the disc, compressive stresses are higher than in the anterior region of the disc for a neutral position of the spine.

In the flexion position, $\boldsymbol{\varepsilon_{max}}$ and $\boldsymbol{\varepsilon_{min}}$ absolute values have increased for the anterior sensors (C5-Anterior and C6-Anterior) while values have decreased for the posterior sensors (C5-Posterior and C6-Posterior) when compared to the neutral position. This is because the flexion movement moves the head forward, increasing the proximity between the anterior area of the vertebral body which increases

tension in that area. This is corroborated by the McNally *et al* and Bonnheim *et al* studies where flexion of the spine created a peak in vertical stress on the anterior region of the IVD which leads to higher deformation in the anterior section of the adjacent vertebrae [43], [45]. The same logic applies to the extended position where the opposite happens since the head moves backward. Compared to the neutral, absolute values of strain increase in the posterior sensors and decrease in the anterior ones for the extended position.

5.2. Strain with the prosthetic disc in the assembly for different positions

Figure 4.3 shows the strain values over time of the various sensors. The behaviour is to be expected with a slow increase in deformation until it peaks when the force applied to the system is 50 N.

As shown in table 4, in the neutral position of the model, the highest absolute values were measured in the C6 vertebra. The lowest values were measured in the C5-Anterior. We can deduce that in this model the force is applied in the majority to the posterior part of the vertebral body.

In the flexion position, all the sensors showed lower absolute values of strain in the posterior area (C5-Posterior and C6-Posterior) and higher values in the C5-Anterior compared to the neutral position, as expected. The C6-Anterior sensor showed lower values which may be due to experimental errors like incorrect positioning of the prosthetic disc since there was a small gap between the Mobi-C disc endplates and the vertebral body. In the extension position, the C6-Posterior showed higher absolute $\boldsymbol{\varepsilon_{max}}$ and $\boldsymbol{\varepsilon_{min}}$ values and C6-Anterior showed lower absolute values as it was expected. However, C5 sensors showed unexpected results which may be caused by experimental errors as mentioned before.

5.3. Comparison of natural and prosthetic disc models

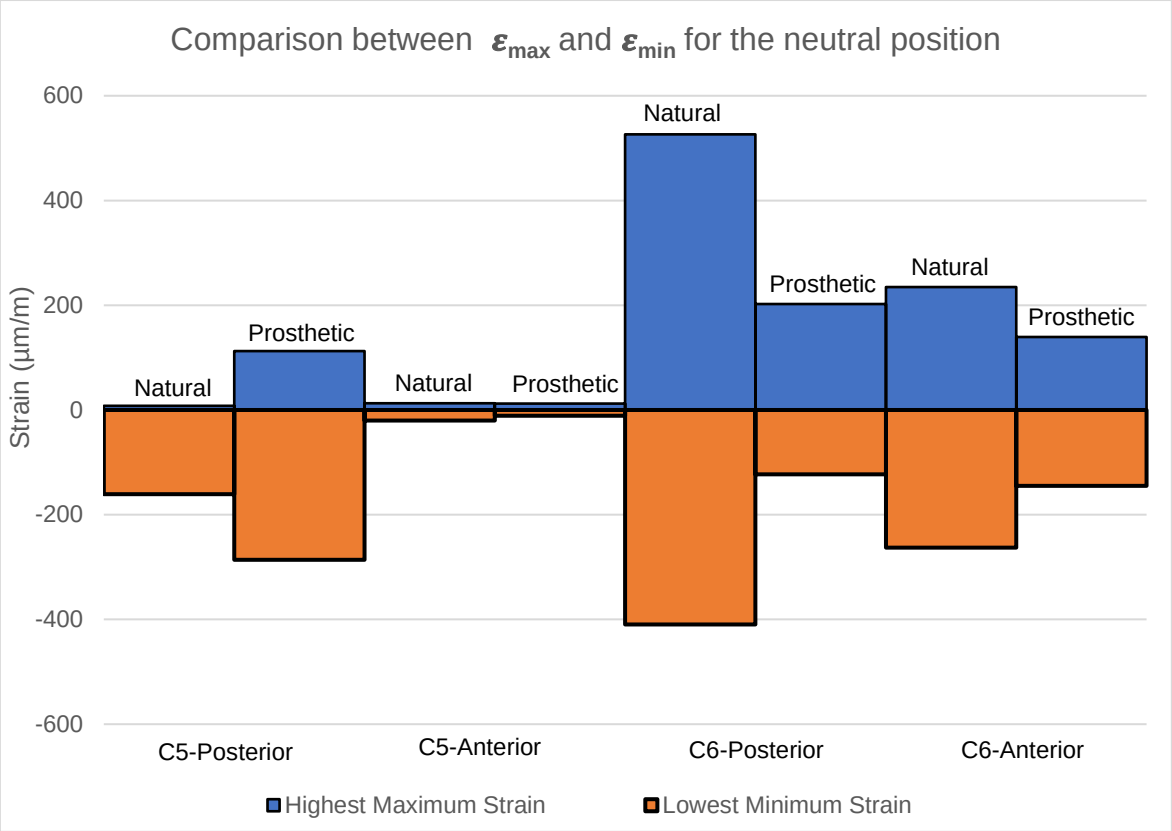

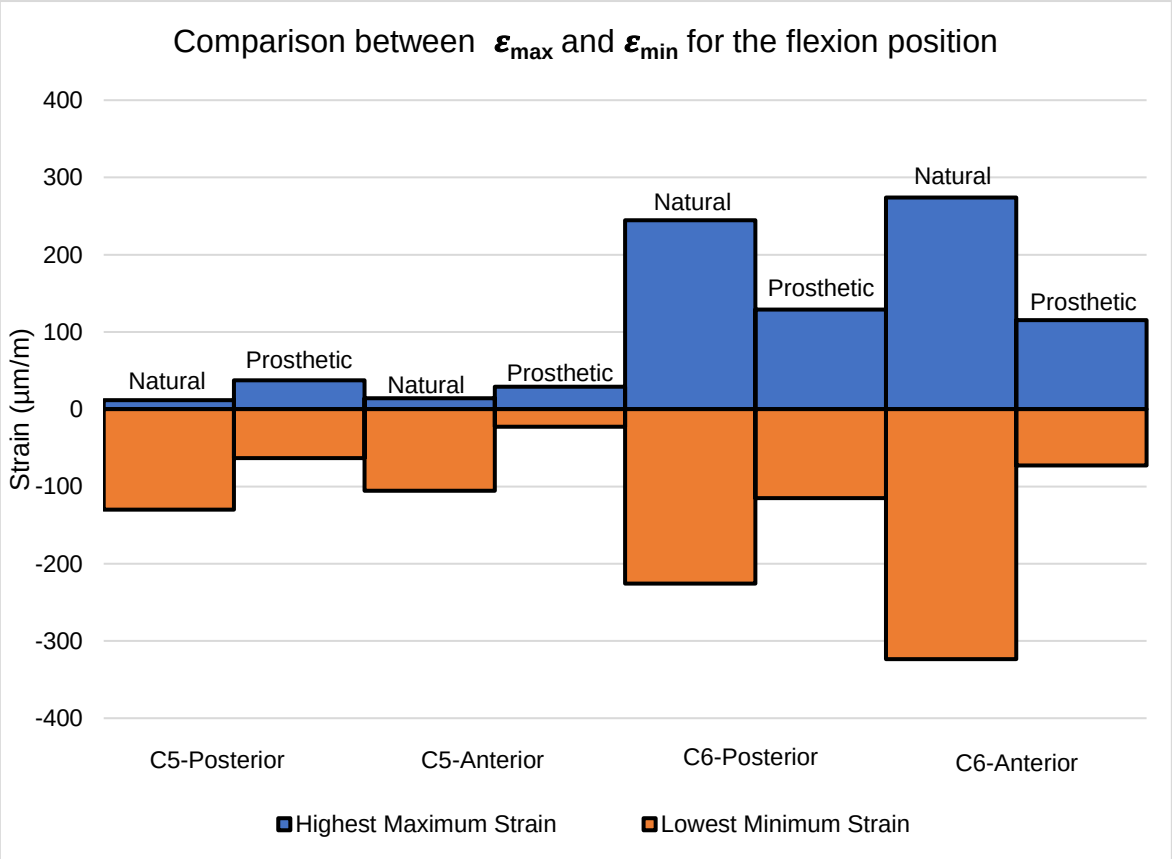

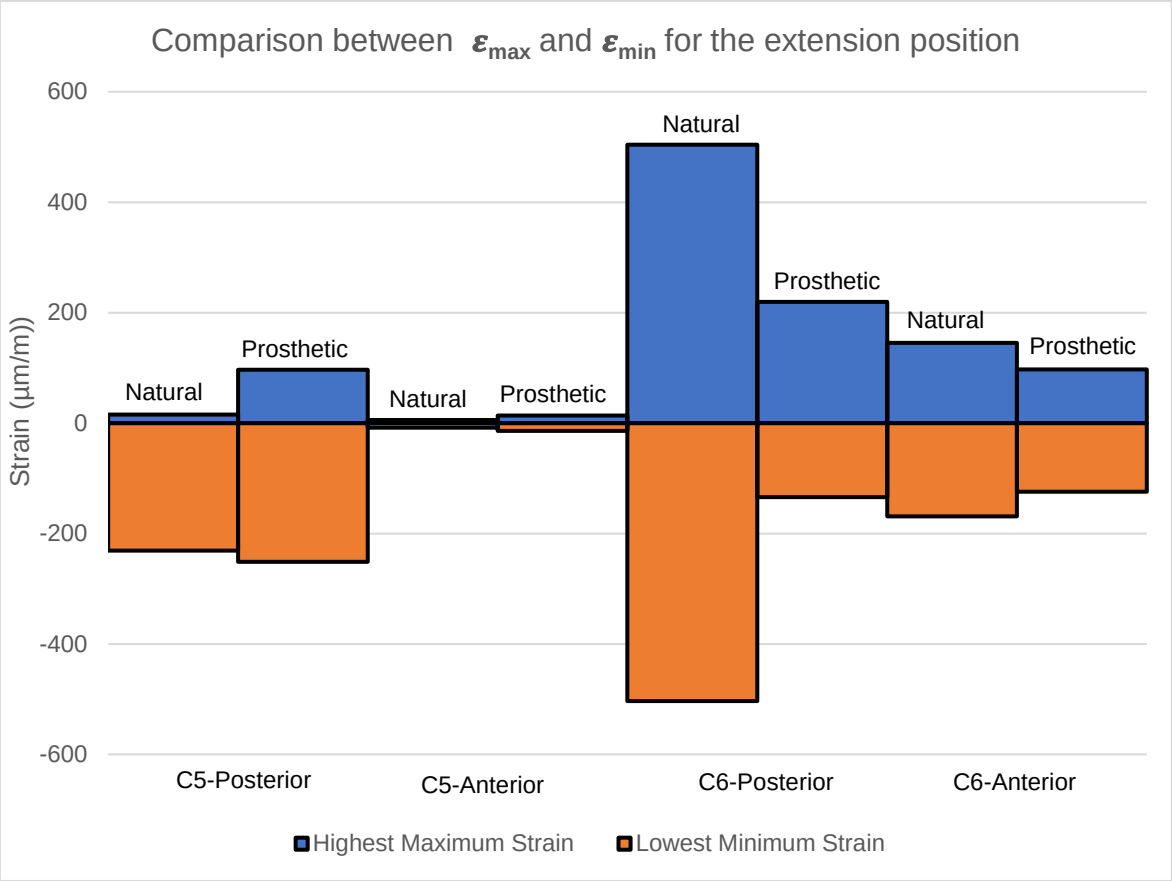

Figure 5.1 Maximum ε_{max} and minimum ε_{min} value comparison for the different positions of the cervical spine.

When comparing the ε_{max} and ε_{min} between the natural and prosthetic disc models as shown in table 4 and figure 5.1, the biggest difference is the highest absolute deformation values which are higher in the natural disc. The overall biggest value measured for ε_{max} was measured in the C6-Posterior with a neutral position and the natural disc (526.40 µm/m). The overall highest absolute value for ε_{min} was also at the C6-Posterior in the extension position with the natural disc (503.58 µm/m). The lowest values for strain were also measured for the natural disc model in the C5-Anterior sensor in the extension position (5.64 and 8.59 µm/m). This indicates that the natural discs distribute the load applied to the system less evenly across the vertebral body than the prosthetic disc in this system. The difference between the highest strain value and the lowest is 520.76 µm/m and 0.59 µm/m for ε_{max} and ε_{min} in the natural disc model and 207.31 µm/m and 274.77 µm/m for ε_{max} and ε_{min} in the prosthetic disc model. The disparity between values in different sensors is noticeably higher in the natural disc than in the prosthetic disc.

Thanks to the geometry and alignment of the prosthetic disc which allows the dispersion of load evenly on the vertebral body without creating stress in certain parts of the model. Bonnheim *et a*l confirms this deduction because the results from the study show that most cervical implants regardless of their overall stiffness properties, will re-distribute stress in a larger portion of the underlying vertebral body [44], [45].

The results show that the artificial disc applies force to the vertebral body more evenly for a neutral position, flexion, and extension than the native disc. This can lead to a higher probability of successful treatment of spinal pathologies and can even help cure the disease restoring full motion to the spine for a period of time.

Chapter 6. Conclusions and Future Work

The results obtained in this work showed that a successful method for testing the spine and IVDs was developed. They confirm that the hardness of an IVD has an integral part in changing the deformation of the adjacent vertebrae which in the long term can affect the development of spinal pathologies. The results also show that most of the load is carried by the posterior area of the vertebral body rather than the anterior part. The main conclusion was that, for this assembly, the prosthetic disc distributes the load of the cervical spine in a more uniform distribution on the vertebral body of the vertebrae than the natural disc model due mainly to its geometry, mechanical properties, and alignment in the developed experimental segment. Of course, the prosthetic disc is not superior to the native one but in this study, it is evident that with proper alignment and setup, the Mobi-C disc applies force to the vertebrae evenly for a neutral position, flexion, and extension. This may show that the prosthetic disc can diminish stress peaks in the adjacent vertebral bodies which can lead to a relief or treatment of spinal pathologies because, when forces are applied unevenly to some parts of the vertebrae, deterioration of the disc and bone can occur and consequently other diseases.

For future work, it is relevant to try to fix the experimental flaws associated with the current experimental models by including more ligaments, and more forces applied from different directions and increase the overall stability of the system. It is possible to also use a cadaveric spinal unit which is a perfect environment for testing disc prostheses. A good idea is to create a separate natural disc with different geometries for the different positions of flexion and extension to minimize gaps and increase the overall reliability of the results. Also, it would be interesting to add other movements to the biomechanical analysis like lateral bending and rotation as well as using other arthroplasty disc devices available in the market today. A biomechanical comparison between different devices and the native is work that would be very useful for the medical community and for the public overall who use disc prosthetic devices to cure disease.

In the end, the main objective of this project accomplished with illustrative results of the biomechanical behaviour in the cervical spine with the native disc and highlighted the importance of disc arthroplasty devices for the spine.

References

[1] C. R. Clark, E. C. Benzel, and C. S. R. S. E. Committee, *The Cervical Spine*. Lippincott Williams \& Wilkins, 2005.

[2] T. Taylor, “Cervical Vertebrae.” https://www.innerbody.com/anatomy/skeletal/cervical-vertebrae-lateral (accessed Oct. 10, 2022).

[3] “Spine Anatomy: Intervertebral Discs.” https://www.sonsa.org/spine-surgery/spine-anatomy/intervertebral-discs/ (accessed Oct. 20, 2022).

[4] T. Lujikx and H. Knipe, “Typical cervical vertebrae,” 2014, [Online]. Available: https://doi.org/10.53347/rID-30852.

[5] J. T. Kaiser, V. Reddy, and J. G. Lugo-Pico, “Anatomy, Head and Neck, Cervical Vertebrae.,” Treasure Island (FL), 2022.

[6] N. Yoganandan, S. Kumaresan, and F. A. Pintar, “Geometric and mechanical properties of human cervical spine ligaments.,” *J. Biomech. Eng.*, vol. 122, no. 6, pp. 623–629, Dec. 2000, doi: 10.1115/1.1322034.

[7] “Measurement of range of motion of the cervical spine and temporomandibular joint.” https://musculoskeletalkey.com/measurement-of-range-of-motion-of-the-cervical-spine-and-temporomandibular-joint/ (accessed Oct. 10, 2022).

[8] D. Carrison and B. Bledsoe, “Why EMS Should Limit the Use of Rigid Cervical Collars,” 2015. https://www.jems.com/patient-care/why-ems-should-limit-use-rigid-cervical/ (accessed Oct. 10, 2022).

[9] N. Bogduk and S. Mercer, “Biomechanics of the cervical spine. I: Normal kinematics.,” *Clin. Biomech. (Bristol, Avon)*, vol. 15, no. 9, pp. 633–648, Nov. 2000, doi: 10.1016/s0268-0033(00)00034-6.

[10] L. Penning, “Normal movements of the cervical spine,” *Am. J. Roentgenol.*, vol. 130, no. 2, pp. 317–326, Feb. 1978, doi: 10.2214/ajr.130.2.317.

[11] J. McAviney, D. Schulz, R. Bock, D. E. Harrison, and B. Holland, “Determining the relationship between cervical lordosis and neck complaints.,” *J. Manipulative Physiol. Ther.*, vol. 28, no. 3, pp. 187–193, 2005, doi: 10.1016/j.jmpt.2005.02.015.

[12] R. Bayoglu, P. Galibarov, N. Verdonschot, B. Koopman, and J. Homminga, “Twente Spine Model: A thorough investigation of the spinal loads in a complete and coherent musculoskeletal model of the human spine,” *Med. Eng. Phys.*, vol. 68, Apr. 2019, doi: 10.1016/j.medengphy.2019.03.015.

[13] M. A. C. Negrelli, R. G. D. E. Oliveira, I. D. D. A. Rocha, A. F. Cristante, R. M. Marcon, and T. E. P. D. E. F. Barros, “Traumatic Injuries of the Cervical Spine: Current Epidemiological Panorama.,” *Acta Ortop. Bras.*, vol. 26, no. 2, pp. 123–126, 2018, doi: 10.1590/1413-785220182602185460.

[14] J. S. Harrop *et al.*, “Lumbar adjacent segment degeneration and disease after arthrodesis and total disc arthroplasty.,” *Spine (Phila. Pa. 1976).*, vol. 33, no. 15, pp. 1701–1707, Jul. 2008, doi: 10.1097/BRS.0b013e31817bb956.

[15] R. W. Bailey and C. E. Badgley, “Stabilization of the cervical spine by anterior fusion.,” *J. Bone Joint Surg. Am.*, vol. 42-A, pp. 565–594, Jun. 1960.

[16] T. F. Fekete and F. Porchet, “Overview of disc arthroplasty-past, present and future,” *Acta Neurochir. (Wien).*, vol. 152, no. 3, pp. 393–404, 2010, doi: 10.1007/s00701-009-0529-5.

[17] T. R. Niedzielak, B. J. Ameri, B. Emerson, R. M. Vakharia, M. W. Roche, and J. P. Malloy IV, “Trends in cervical disc arthroplasty and revisions in the Medicare database,” *J. Spine Surgery; Vol 4, No 3 (September 2018) J. Spine Surg.*, 2018,

[Online]. Available: https://jss.amegroups.com/article/view/4290.
[18] D. Coric and P. V. Mummaneni, “Nucleus replacement technologies: Invited submission from the Joint Section Meeting on Disorders of the Spine and Peripheral Nerves, March 2007,” *J. Neurosurg. Spine*, vol. 8, no. 2, pp. 115–120, 2008, doi: 10.3171/SPI/2008/8/2/115.
[19] T. J. Errico, “Lumbar disc arthroplasty.,” *Clin. Orthop. Relat. Res.*, no. 435, pp. 106–117, Jun. 2005, doi: 10.1097/01.blo.0000165718.22159.d9.
[20] K. Büttner-Janz, K. Schellnack, and H. Zippel, “Biomechanics of the SB Charité lumbar intervertebral disc endoprosthesis.,” *Int. Orthop.*, vol. 13, no. 3, pp. 173–176, 1989, doi: 10.1007/BF00268042.
[21] S. Lu *et al.*, “An 11-year minimum follow-up of the Charite III lumbar disc replacement for the treatment of symptomatic degenerative disc disease.,” *Eur. spine J. Off. Publ. Eur. Spine Soc. Eur. Spinal Deform. Soc. Eur. Sect. Cerv. Spine Res. Soc.*, vol. 24, no. 9, pp. 2056–2064, Sep. 2015, doi: 10.1007/s00586-015-3939-5.
[22] P. Tropiano, R. Huang, F. Girardi, and T. Marnay, “Lumbar Disc Replacement,” *Spine (Phila. Pa. 1976).*, vol. 28, pp. 362–368, Aug. 2003, doi: 10.1097/00007632-200300001-00008.
[23] N. Plais, X. Thevenot, A. Cogniet, J. Rigal, and J. C. Le Huec, “Maverick total disc arthroplasty performs well at 10 years follow-up: a prospective study with HRQL and balance analysis.,” *Eur. spine J. Off. Publ. Eur. Spine Soc. Eur. Spinal Deform. Soc. Eur. Sect. Cerv. Spine Res. Soc.*, vol. 27, no. 3, pp. 720–727, Mar. 2018, doi: 10.1007/s00586-017-5065-z.
[24] R. C. Sasso, D. M. Foulk, and M. Hahn, “Prospective, randomized trial of metal-on-metal artificial lumbar disc replacement: initial results for treatment of discogenic pain.,” *Spine (Phila. Pa. 1976).*, vol. 33, no. 2, pp. 123–131, Jan. 2008, doi: 10.1097/BRS.0b013e31816043af.
[25] A. T. Villavicencio, S. Burneikiene, R. Pashman, and J. P. Johnson, “Spinal Artificial Disc Replacement : Cervical Arthroplasty Part II : Indications , Surgical Technique , and Complications,” vol. 29, no. 13, pp. 1–6, 2007.
[26] “Artificial Disc Replacement.” https://www.adrspine.com/artificial-disc-replacement/cervical-disc-replacement (accessed May 23, 2022).
[27] “Biomechanics of Lumbar Disk Arthroplasty.” https://musculoskeletalkey.com/biomechanics-of-lumbar-disk-arthroplasty/ (accessed May 23, 2022).
[28] “MAVERICK Total Disc Replacement.” https://plasticsurgerykey.com/maverick-total-disc-replacement/ (accessed May 23, 2022).
[29] J.-M. Vital and L. Boissière, “Total disc replacement,” *Orthop. Traumatol. Surg. Res.*, vol. 100, no. 1, Supplement, pp. S1–S14, 2014, doi: https://doi.org/10.1016/j.otsr.2013.06.018.
[30] Q.-B. Bao, G. M. Mccullen, P. A. Higham, J. H. Dumbleton, and H. A. Yuan, “The artificial disc: theory, design and materials,” *Biomaterials*, vol. 17, no. 12, pp. 1157–1167, 1996, doi: https://doi.org/10.1016/0142-9612(96)84936-2.
[31] S. S. Gill and C. Walker, “United States Patent No. 6,113,637,” 2000.
[32] N. Duggal, D. R. Baker, and R. Conta, *United States Patent No. 8,231,677 B2*, vol. 2, no. 12. 2012.
[33] F. Gauchet, “United States Patent Gauchet No. 6,395,032 B1,” 2002.
[34] Y. Kotani *et al.*, “Artificial intervertebral disc replacement using bioactive three-dimensional fabric: design, development, and preliminary animal study.,” *Spine (Phila. Pa. 1976).*, vol. 27, no. 9, pp. 926–929, May 2002, doi: 10.1097/00007632-200205010-00008.
[35] M. Putzier *et al.*, “Charité total disc replacement--clinical and radiographical results

after an average follow-up of 17 years.," *Eur. spine J. Off. Publ. Eur. Spine Soc. Eur. Spinal Deform. Soc. Eur. Sect. Cerv. Spine Res. Soc.*, vol. 15, no. 2, pp. 183–195, Feb. 2006, doi: 10.1007/s00586-005-1022-3.

[36] K. Radcliff *et al.*, "Long-term Evaluation of Cervical Disc Arthroplasty with the Mobi-C© Cervical Disc: A Randomized, Prospective, Multicenter Clinical Trial with Seven-Year Follow-up.," *Int. J. spine Surg.*, vol. 11, no. 4, p. 31, 2017, doi: 10.14444/4031.

[37] K. Kim *et al.*, "Ten-Year Outcomes of 1- and 2-Level Cervical Disc Arthroplasty From the Mobi-C Investigational Device Exemption Clinical Trial.," *Neurosurgery*, vol. 88, no. 3, pp. 497–505, Feb. 2021, doi: 10.1093/neuros/nyaa459.

[38] Zimmer Biomet, "Surgical Technique Guide" 2012 https://www.zimvie.com/en/spine/cervical-solutions/mobi-c-cervical-disc.html (accessed Oct. 05, 2022).

[39] "Mobi-C Cervical Disc Brochure" 2018. https://www.zimvie.com/en/spine/cervical-solutions/mobi-c-cervical-disc.html (accessed Jul. 22, 2022).

[40] J. L. Pinheiro-Franco, A. R. Vaccaro, E. C. Benzel, and H. M. Mayer, *Advanced Concepts in Lumbar Degenerative Disk Disease*. 2016.

[41] M. H. Pham, V. A. Mehta, A. Tuchman, and P. C. Hsieh, "Material Science in Cervical Total Disc Replacement.," *Biomed Res. Int.*, vol. 2015, p. 719123, 2015, doi: 10.1155/2015/719123.

[42] J. A. A. Miller, A. B. Schultz, D. N. Warwick, and D. L. Spencer, "Mechanical properties of lumbar spine motion segments under large loads," *J. Biomech.*, vol. 19, no. 1, pp. 79–84, 1986, doi: https://doi.org/10.1016/0021-9290(86)90111-9.

[43] D. S. McNally and M. A. Adams, "Internal intervertebral disc mechanics as revealed by stress profilometry.," *Spine (Phila. Pa. 1976).*, vol. 17, no. 1, pp. 66–73, Jan. 1992, doi: 10.1097/00007632-199201000-00011.

[44] P. A. Cripton, "Load-sharing in the human cervical," 1999.

[45] N. B. Bonnheim and T. M. Keaveny, "Load-transfer in the human vertebral body following lumbar total disc arthroplasty: Effects of implant size and stiffness in axial compression and forward flexion.," *JOR spine*, vol. 3, no. 1, p. e1078, Mar. 2020, doi: 10.1002/jsp2.1078.

[46] "SAWBONES Orthopaedic models." ttps://www.sawbones.com/catalog/orthopaedic-models.html?character11=121&p=3 (accessed Oct. 05, 2022).

[47] "PolyJet 3D Printing." https://www.protolabs.com/services/3d-printing/polyjet/ (accessed Sep. 05, 2022).